THE CALIBRATION OF A CURVED CRYSTAL GAMMA-RAY SPECTROMETER USING A RADIOACTIVE SOURCE OF Ir-192

A Thesis submitted in partial fulfilment of the requirements for the degree of Master of Science at the University of Manitoba

THE UNIVERSITY OF MANITOBA LIBRARY

by

John F. Moore

October, 1959

PREFACE

The work presented in this thesis was carried out at the University of Manitoba during May 1958 - September 1959 under the direction of Dr. D. G. Douglas.

The author wishes to express his gratitude to Dr. D. G. Douglas without whose supervision this project could not have been undertaken and to Dr. R. D. Connor for his invaluable discussions on the gamma-ray spectrum of Ir-192. Acknowledgement is also due for Miss B. Hartland for accepting all typing work.

ABSTRACT

A transmission type curved crystal spectrometer has been constructed at the University of Manitoba. The spectrometer employs a quartz crystal, 1 millimeter thick and bent to a radius of 1.24 meters.

The following thesis contains a description of the instrument, a detailed account of its alignment, and the calibration results obtained using a radioactive source of Ir-192. A curve is derived calibrating the driving mechanism of the spectrometer in terms of wavelength. The precision in the determination of the proportionality constant linking dial setting with wavelength is shown to be one part in five thousand for the energy region below 200 kev. and one part in eight hundred for the region above 200 kev. A tentative explanation for the reduction in precision is offered and several defects in alignment procedure are considered.

An empirical curve is derived in an attempt to resolve the radical disagreement between Johns and Baggerly over the relative photon intensities of certain gamma-ray transitions following the decay of Ir-192. This curve would seem to indicate that Baggerly's values of 1.8 and 39 for the relative photon intensities of the 136 kev. and 485 kev. transition respectively are correct to within at least 20%.

CONTENTS

Chapter Page

1. Introduction

(I) Historical Introduction ---------- 1

(II) Theoretical Introduction -------- 4

2. Design of the Spectrometer

(I) Operational Features ---------- 10

(II) Source and Source Mount Design --- 17

(III) Crystal Clamping Arrangement ---- 23

(IV) Collimator ---------- 26

(V) Detector System ---------- 29

3. Alignment of the Spectrometer

(I) Preliminary Mechanical Alignment -- 33

(II) Final Alignment ---------- 51

4. Investigation of the Gamma-Ray and X-ray Spectra of Ir-192

(I) Introduction ---------- 64

(II) Procedure ---------- 71

(III) Results ---------- 73

5. Discussion of Results

(I) Performance of the Spectrometer --- 88

(II) Gamma-ray Spectrum of Ir-192 ----- 93

Bibliography ---------- 95

List of Figures and Plates

Fig. (1) Principle of curved crystal reflection -------- 5

Fig. (2) Dumond's exact solution ---------- 5

Fig. (3) Cauchois(approximate solution ---------- 8

Fig. (4) Geometry of the spectrometer ---------- 11

Fig. (5) Perspective line drawing of the spectrometer - 12

Plate (1) Over-all view of the spectrometer ---------- 13

Fig. (6) Source capsule ---------- 19

Fig. (7) Source castle ---------- 19

Fig. (8) Remote control assembly ---------- 22

Fig. (9) Quartz crystal with enclosing template --------25

Plate (2) Crystal clamping assembly ---------- 25

Fig.(10) Perspective line drawing of the main collimator - 28

Fig.(11) Detector head assembly ---------- 30

Fig.(12) Block diagram of the scintillation spectrometer - 30

Fig.(13) Rack characteristics ---------- 36

Fig.(14) Spindle alignment ---------- 42

Fig.(15) Transmission characteristics of the main collimator - 49

Fig.(16) Vertical orientation of the crystal planes --- 56

Fig.(17) Source orientation ---------- 58

Fig.(18) Decay scheme of Ir-192 according to Baggerly - 65

Fig.(19) Gamma-ray spectrum of Ir-192 ---------- 74

Fig.(20) Intense Platinum triad ---------- 76

Fig.(21) Comparison between typical gamma-ray and X-ray peaks - 77

Fig.(22) Wavelength calibration curve ---------- 81

Fig.(23) Intensity calibration curve ---------- 87

Fig.(24) Geometry of the spectrometer showing possible misalignment ---------- 89

GLOSSARY

The following is a glossary of terms and symbols used in the description of the mechanical features of the curved crystal spectrometer. For clarification the reader is referred to figures (4) and (5).

Spindle B'	the thrust bearing about which the track T rotates in a horizontal plane
Spindle O	the spindle which links the source carriage R to radial beam II. This spindle defines the centre of the Rowland circle.
Spindle C_1	the spindle about which radial beam I rotates.
Spindle C_2	the spindle about which radial beam II rotates. N.B. the axes of spindles C_1 and C_2 are collinear.
Radial beam I	the physical realization of the line CR' in figure (4).
Radial beam II	the physical realization of the line CB in figure (4).
Radius bar I	the physical realization of the line OR in figure (4). This bar provides a rigid link between the source carriage and spindle O.
Radius bar II	the rigid bar which links the spindle O to the spindle C_1.
Carriage L	the carriage which supports the un-pivoted end of radial beam I.

Carriage R	the carriage which supports the source castle.
Carriage Q	the carriage upon which L travels.
Track T	the track upon which Q travels

Chapter 1 - Introduction

(I) HISTORICAL INTRODUCTION

The study of X-ray spectra by means of crystalline diffraction was carried on for many years before the identification of electromagnetic radiation from radio-active nuclei by Ellie in 1922. The principal method used was the rotating crystal technique of Bragg[1]. This technique was first applied to the study of gamma-ray spectra by Frilley[2] and by Thibaud[3]. Frilley's spectrometer, which employed Bragg surface reflection at grazing angles from a flat crystalline lamina, had several disadvantages, the two most serious being the low resolving power for short wavelengths and the necessity for using a very intense line source which tended to mask the selectively reflected spectrum.

A curved crystal focusing X-ray spectrometer technique was first suggested by Dumond[4] in 1930 and first realized practically by Cauchois[5] in 1932. Very little attention, however, was paid to the adaptation of this method to the investigation of gamma-ray spectra until 1947. In this year Dumond[6] constructed a curved crystal spectrometer with a view to making accurate determinations of the wavelengths of high energy gamma-rays by direct crystal diffraction. Since then he has published several papers[6-12] on the precision measurements of gamma-ray wavelengths.

Dumond's spectrometer employs a quartz crystal, 2 mm. in thickness, with a radius of curvature of 2 metres

and an aperture of dimensions 1.7 x 2 inches. With this machine he has made an extensive investigation of the gamma-ray spectrum of several isotopes. His latest paper[12] on Ir-192 quotes a half width of 0.25 mA for the lines observed in the spectrometer. The errors assigned to the energies of the determined gamma-rays correspond to one twentieth of this line width except for the weaker lines where the error corresponds to one fifth of the line width. To date, Dumond has been unable to resolve the 605 kev and 613 kev lines of Ir-192 without using the method of composite profiles[13].

Various other transmission-type curved crystal spectrometers[14,15,16] have been constructed since 1947, most of which use an arrangement of source and detector similar to that of Dumond. In this arrangement the spectrum from a line source is explored point by point, and the intensity, measured by means of a scintillation counter, is plotted as a function of source position. The alternative arrangement, which is essentially the transmission photographic spectrometer of Cauchois, records an entire spectral region simultaneously on a film, and makes use of an extended source. For high energy work Dumond's arrangement is the superior since it removes the problem of shielding the film from the intense direct beam, while at longer wavelengths, where the radiation intensity is such that photographic spectra can be taken with reasonable exposure times, Cauchois' arrangement has the advantage in exploratory work, a considerable segment of the spectrum being explored in a single exposure.

Dumond[17] has pointed out the advantages and disadvantages of the study of gamma-ray spectra by direct crystal diffraction relative to the indirect study by "conversion" spectrometry. The disadvantages are; the need for much more intense line sources, the fact that the use of small solid angles from the source makes coincidence work impossible, and the lack of any information on the multipolarity of the gamma-ray transitions. On the other hand, crystal diffraction has several advantages over beta-ray spectrometry. Sources are much easier to prepare. The gamma-ray energies can be measured more precisely. The resolving power of the curved crystal spectrometer is much higher for low energies. Also, the complex pattern of lines of the "conversion" spectrum is avoided in crystal diffraction technique, thus making the interpretation of the gamma-spectrum a much easier task.

A review of the literature to date reveals the curved crystal spectrometer to be a very useful tool in the investigation of the de-excitation of radio-active nuclei. Not only does it afford a series of precisely determined points in the gamma-ray spectrum, but moreover possesses great advantages as an exploratory instrument in both high and low energy regions, thus facilitating the correction and enlargement of many nuclear decay schemes.

(II) THEORETICAL INTRODUCTION

In order to help the understanding of the spectrometer the relevant theory will be discussed in this section. It is largely based on the early papers of Dummond[4] which give a full account of the mode of operation of a transmission type curved crystal spectrometer.

(a) General Theory:

Fundamentally the problem consists of applying the principle of the Rowland concave grating to the case of gamma-ray spectroscopy.

Consider the two-dimensional case as shown in figure (1). A is a point source of composite gamma-rays and B is a point image of a narrow wavelength band $\Delta\lambda$ of wavelength λ in the spectrum of source A. The problem is to find a surface CC' such that a flexible crystal conforming to it would, by Bragg reflection over an extended arc, take gamma-radiation from A and focus it selectively at B. This imposes two conditions at every point on the surface.

(i) at all points on the surface the angles of incidence and reflection referred to the atomic planes must be equal.

(ii) at all points on the surface the angle of deviation ϕ of the reflected beam must be constant for any given wavelength and is given by $\phi = 2 \sin^{-1} (n\lambda/2d)$.

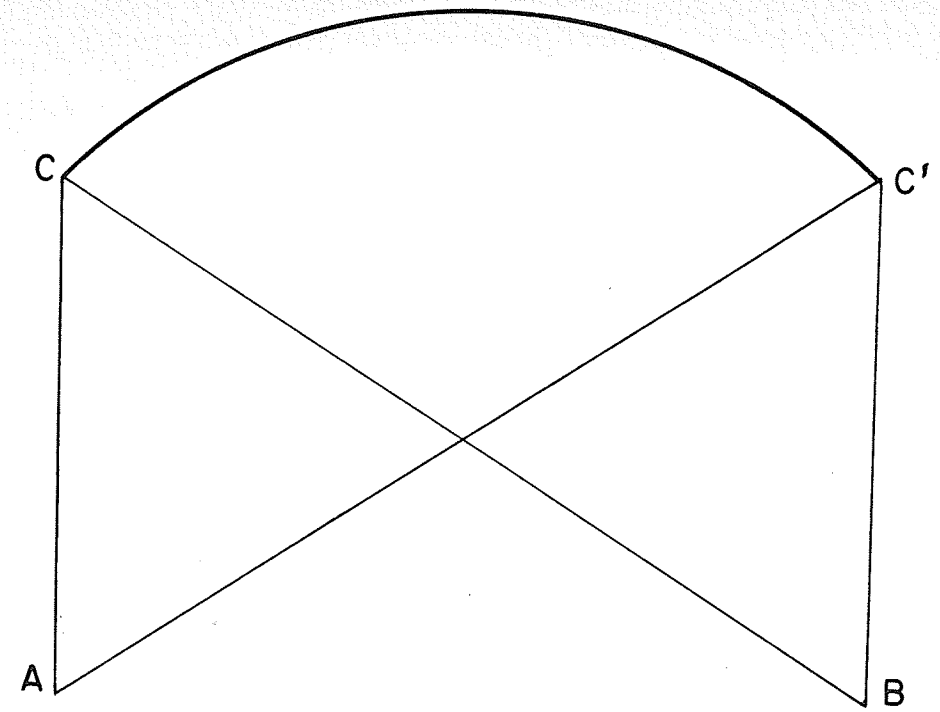

FIG. 1 PRINCIPLE OF CURVED CRYSTAL REFLECTION

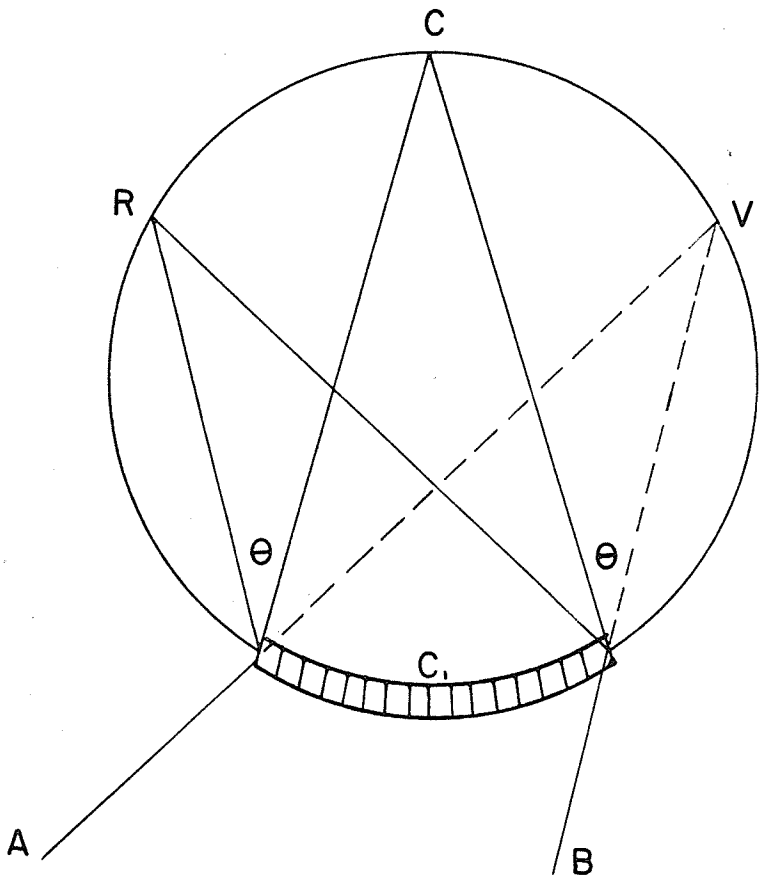

FIG. 2 DUMOND'S EXACT SOLUTION

Condition (i) dictates only the direction of the atomic reflecting planes and imposes no condition on the boundary surface, while condition (ii) dictates the position of every point on the surface but places no condition on the atomic reflecting planes. Thus by suitably profiling the surface and simultaneously bending the crystal it is possible to satisfy both conditions and theoretically obtain perfect focusing.

Figure (2) shows the realization of a crystal bent to satisfy these conditions. In this, the transmission case, the neutral axis of the bent crystal coincides with the focusing circle. The short reflecting planes traversing the crystal, if produced, would intersect at C diametrically opposite to C_1. This case corresponds to a virtual image of the source at V which is realized physically either by a concentrated source at R or by an extended source AB.

The exact solution described above is difficult to obtain. There is, however, an approximate solution which was devised by Cauchois. It should be noted that condition (ii), governing the <u>position</u> of the atomic planes is less stringent than condition (i), governing the <u>direction</u> of the atomic planes. Thus, if a spectrometer is constructed conforming to the latter condition only, a geometrical aberration will be introduced, which will be very small provided the crystal aperture is not too large.

The approximate solution will now be considered in more detail.

(b) Cauchois Approximation:

The previous section considered the case where the reflecting planes used were normal to the unstressed crystal slab, so that they pointed towards the centre of curvature of the bent crystal. The more general case of oblique planes inclined at an angle α to the normals will be considered.

In figure (3) CC' is an extremely thin crystal lamina bent so as to assume a circular section of radius of curvature R and centre of curvature O. The transverse atomic planes are inclined at an angle α to the normals to the crystal slab and intersect at P when produced.

Let ACI be a ray of wavelength λ from an extended source, incident on an atomic plane at C at an angle ϕ such that the Bragg reflection condition, $n\lambda = 2d \sin \phi$, is satisfied. Only rays of wavelength satisfying this condition will be reflected at angle ϕ.

$$\text{Let } u = \hat{OCI} = \phi - \alpha$$

$$\text{and } \theta = \hat{DOC}$$

Consider O as centre of co-ordinates. C will be the point

$$x = - R \sin \theta$$

$$y = R \cos \theta$$

CI will make an angle of $(\pi/2 + u + \theta)$ with the x-axis and its equation is

$$(y - R \cos \theta) - (x + R \sin \theta) \tan (\pi/2 + u + \theta) = 0$$

or

$$(y - R \cos \theta) \tan (u + \theta) + (x + R \sin \theta) = 0 \qquad \text{--- (1)}$$

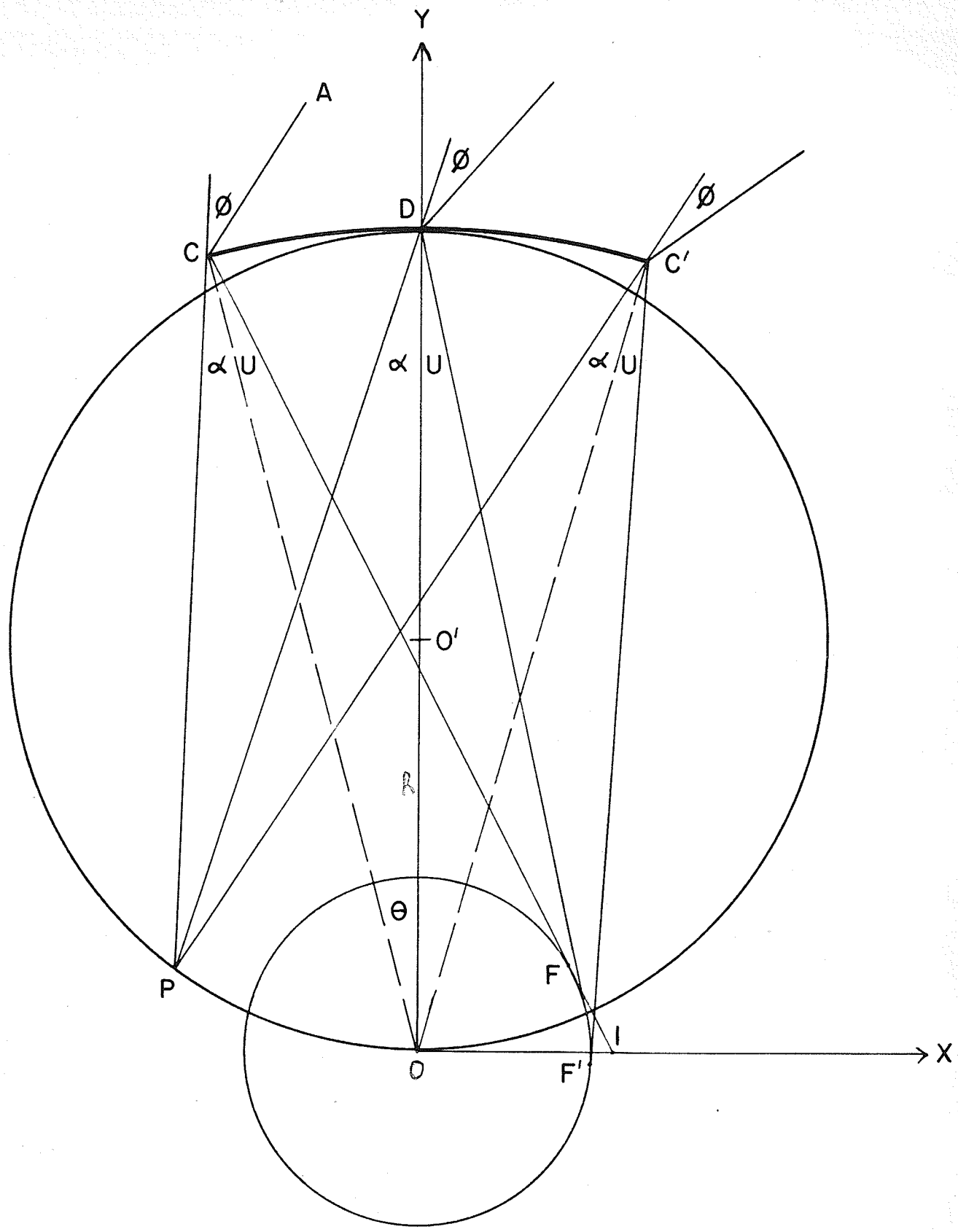

FIG. 3 CAUCHOIS' APPROXIMATE SOLUTION

It is required to find the locus of the intersection of the rays from the source which strike the crystal CC' at this angle ϕ and at positions corresponding to different values of θ. Differentiating (1) with respect to θ and solving for x and y using the equation obtained along with equation (1) gives

$$x = R \sin u \cos (u + \theta)$$

$$y = R \sin u \sin (u + \theta)$$

If the aperture CC' is limited, then the locus of intersection is the arc FF' of a circle of radius R sin u and centre O, the intersecting rays being tangents to the circle.

If the aperture is small enough so that $\theta \approx 0^{\circ}$ then the rays intersect at the point

$$x = R \sin u \cos u$$

$$y = R \sin^2 u$$

The locus of points for different values of ϕ (or u), and so corresponding to rays of different wavelengths, will be a circle of equation

$$x^2 + (y - R/2)^2 = R^2/4$$

whose centre has the coordinates

$$\left.\begin{aligned} x &= 0 \\ y &= R/2 \end{aligned}\right\} \text{i.e. O' of figure (3)}$$

This circle is known as the focusing, or Rowland, circle and if we have a composite source of gamma-rays, rays of different wavelengths will be focused along the circumference of this circle.

Chapter 2 - Design of the Spectrometer

(I) OPERATIONAL FEATURES

As is obvious from figure (2), when the source R moves along the circumference of the focal circle, the direction of the selectively reflected beam changes. Rather than have the extremely difficult task of moving the heavy collimator and detecting system, Dumond[6] devised an arrangement whereby the direction of the reflected beam remains constant. This system was incorporated into the spectrometer under consideration.

As seen in figure (4), the reflected beam is maintained in a fixed direction by rotating the crystal, and consequently the focal circle, about the centre C of the neutral axis of the curved crystal, while simultaneously constraining the source to move along the circumference of the focal circle in such a way that the line joining the source with point C rotates at twice the rate with which the crystal is rotating. The virtual image point V will then remain in a fixed position directly opposite the collimator A.

To fully describe the physical realization of the above system it will be necessary to examine both figures (4) and (5), to which the same reference letters apply. Figure (5) is a perspective line drawing of the spectrometer. Figure (4b) shows the geometry of the instrument in the "zero" position. Figures (4a) and (4c) show the geometry of the machine at its two extremities of travel.

It should be noted that this ability to study the spectra resulting from reflection on either side of the

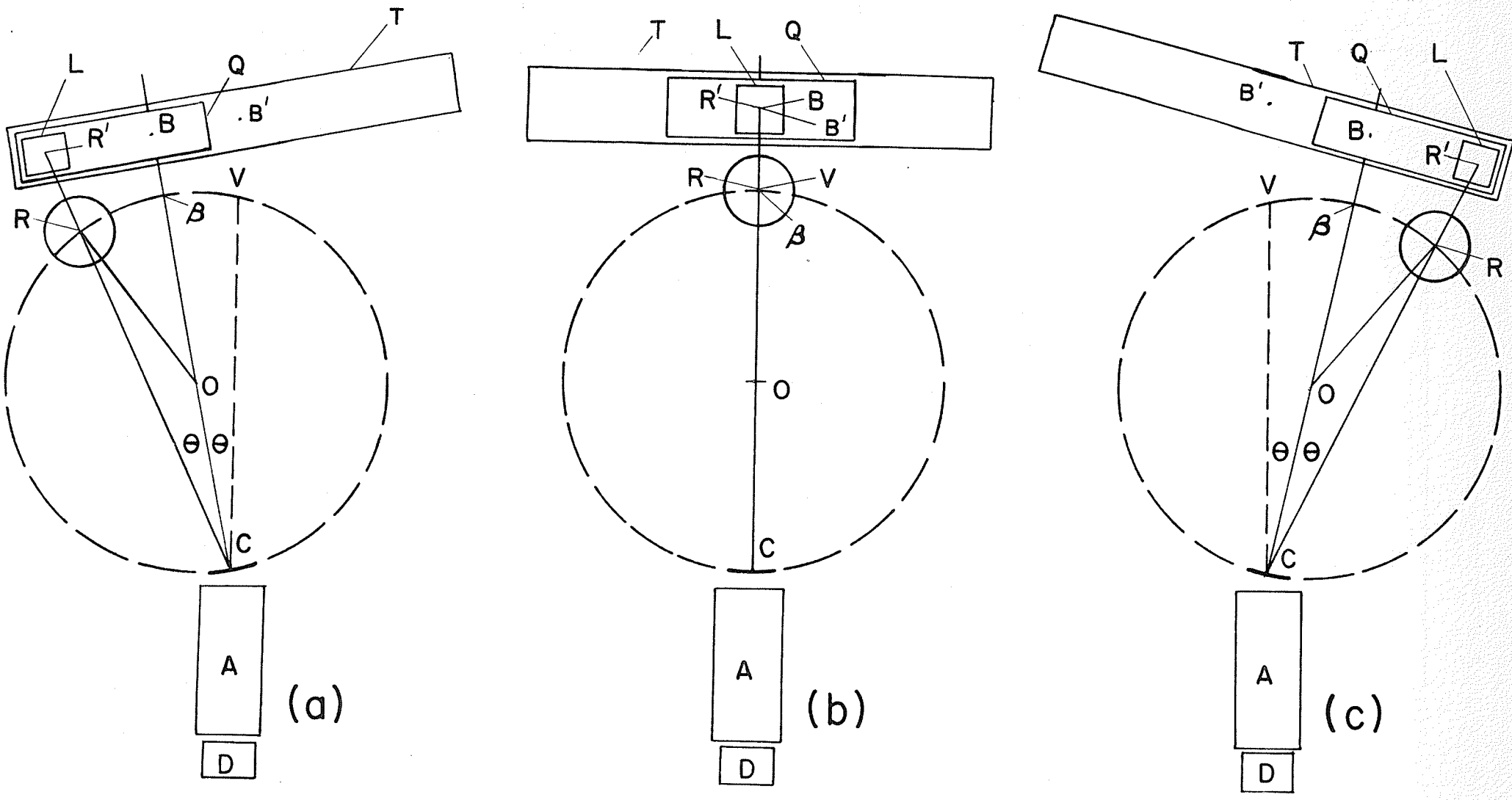

FIG. 4 GEOMETRY OF THE SPECTROMETER

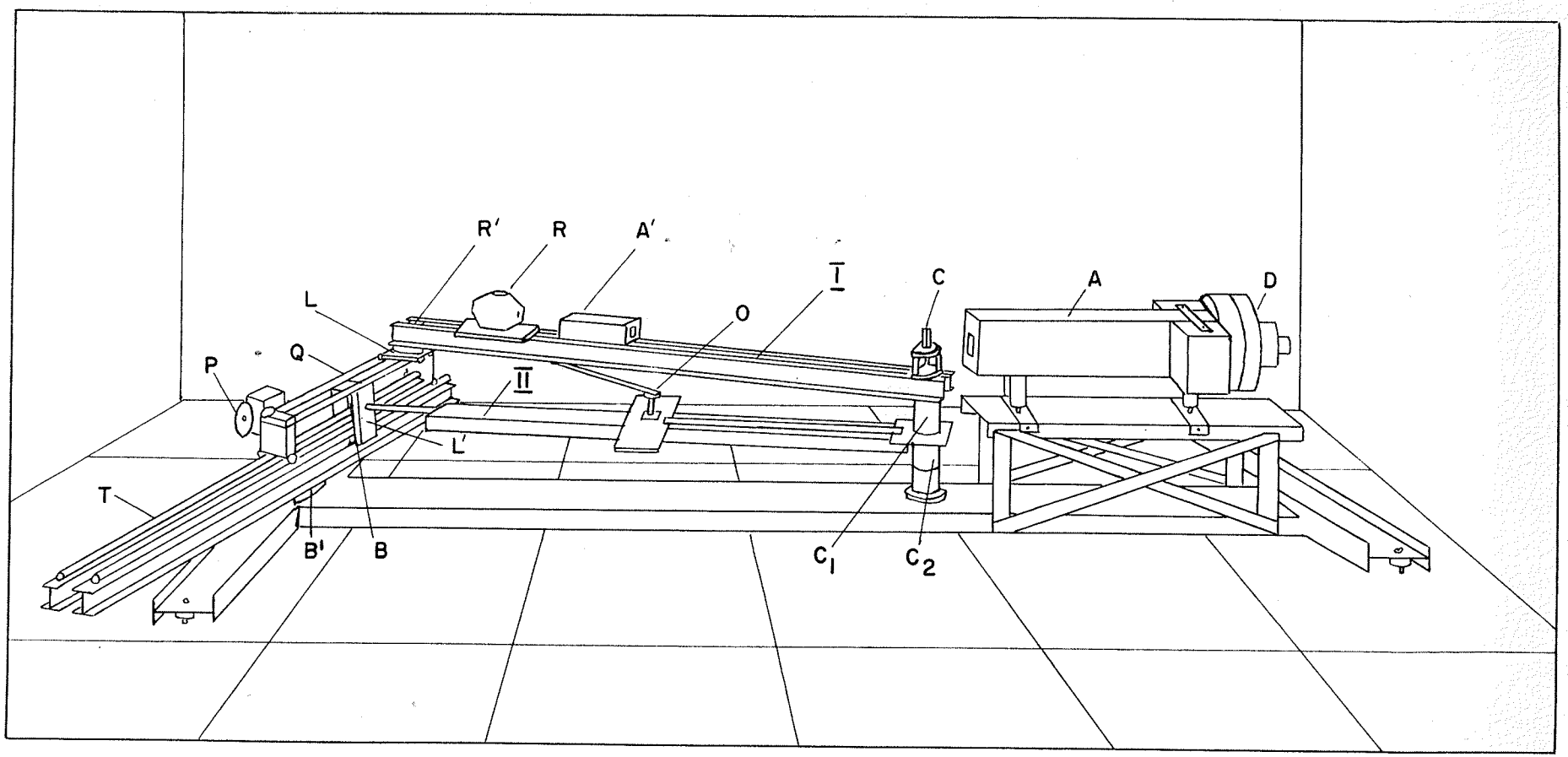

FIG. 5 PERSPECTIVE LINE DRAWING OF THE SPECTROMETER

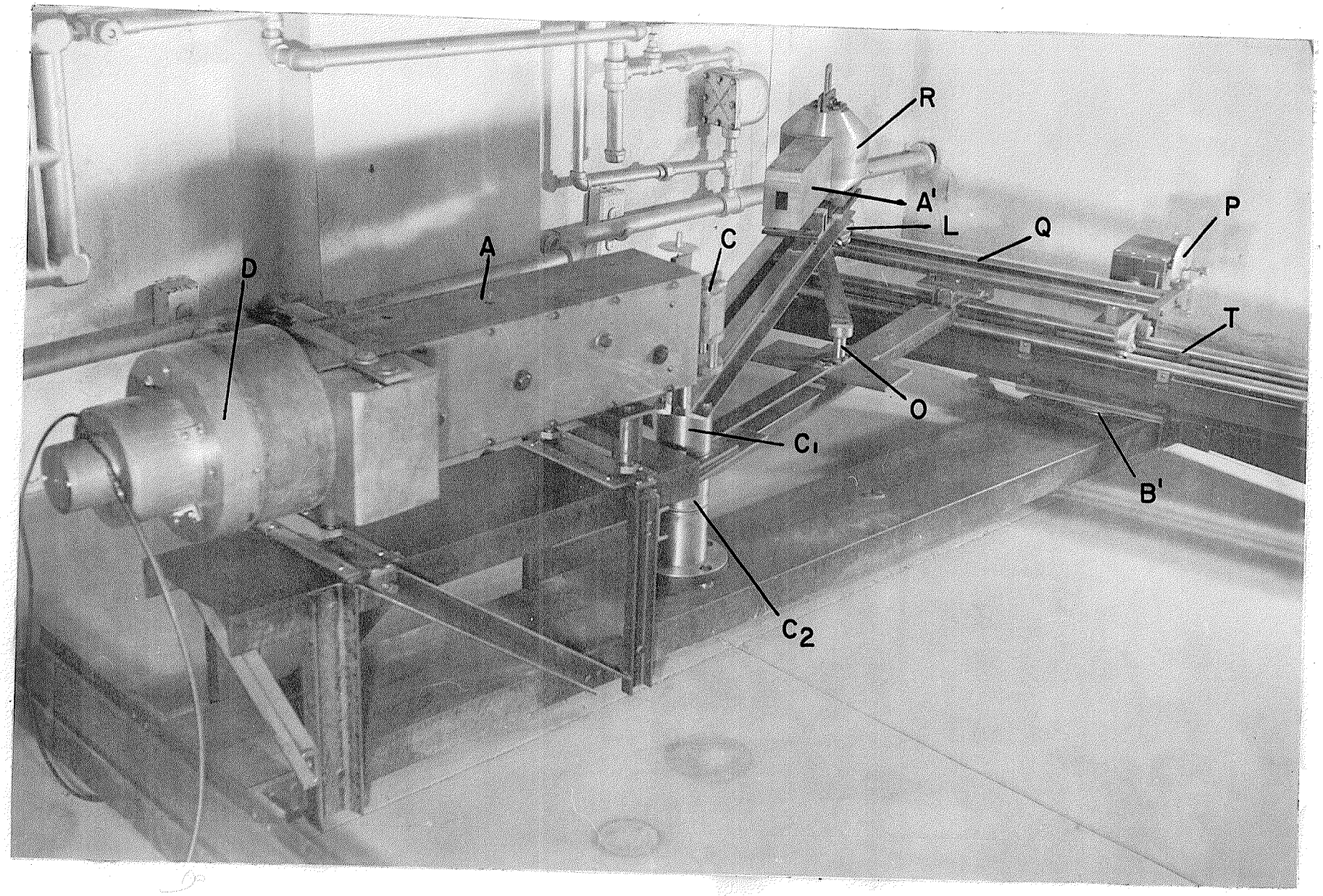

PLATE I OVER-ALL VIEW OF THE SPECTROMETER

transverse planes of the crystal removes the need for knowing beforehand the exact position of β, the "zero" of the wavelength scale.

The focal circle diameter of the spectrometer is 1.24 meters and is physically defined by a radius bar OR which joins the source carriage R, on the upper radial beam CR', to the pivot O defining the centre of the focal circle. The upper radial beam I, constructed of two channel sections held apart by spacers, is pivoted in such a way that it can swing, independently of the crystal holder and lower radial beam II, in a horizontal arc about the point C. The source carriage rides on top of this beam on steel ball bearing ways, and can travel a short distance along the length of the beam as dictated by the motion of the radius bar I. Directly in front of the source carriage is a small collimator A' which acts as a directional device for the intense beam of radiation incident on the crystal. The lower radial beam is also pivoted at C, at a different height above the base, so that it can swing in a horizontal arc. The lower beam, however, is rigidly clamped to the crystal holder by means of a vertical shaft which passes down through the cylindrical steel bearing for the upper beam.

The unpivoted end of the upper radial beam rests on a small carriage L which is free to move on steel roller bearings on the lower carriage Q constructed of two lengths of 1 in. diameter steel shafting held apart by spacers. In turn, the lower carriage is free to move on a track T

which consists of two lengths of 1.19 in. diameter steel shafting clamped securely to two separated channel sections. Since the distance CB [figure (4)] must be capable of variation, the unpivoted end of the lower radial beam terminates in a length of cylindrical steel shafting which rides on roller bearings through a support L' in carriage Q. The track T can swing in a horizontal plane about a 7.09 in. diameter cylindrical steel thrust bearing B' on the base of the machine. CB is the perpendicular bisector of the line R'B'.

The carriage Q is provided with a hardened steel saw-tooth rack, and the track T is geared to this carriage by means of a steel spur gear which, passing through a steel upright on the track, engages in the rack. This rack and pinion system allows the carriage to be driven along the track by the turning of a circular brass disc P which is geared down in a ratio of fifty to one. As the lower carriage Q is driven along the track, the upper carriage L, and consequently the end of the radial beam, is constrained by means of a pulley system to move along the lower carriage in the same direction but at twice the rate. The pulley assembly consists of two steel pulleys, one anchored to each end of the carriage Q. Around the pulleys run two parallel belts of steel piano wire whose ends are clamped to the steel upright from the track T and to the centre of the small carriage L. Any backlash in the system is removed by means of a heavy spring stretched between a variable extension on the track T and the opposite end of the carriage Q. The spring is of such a length that it is under tension

at all times no matter what the relative positions of the track and carriage.

It will be of interest at this point to make a comparison with Dumond's driving assembly. Dumond's carriage is displaced by means of two horizontal longitudinal precision screws located inside the carriage Q. These screws, one situated vertically above the other, are geared together with equal gears so that they rotate at equal rates in opposite senses. The upper screw drives the carriage L while the lower screw drives carriage Q along the track. Compared with a simple pulley system, Dumond's assembly is a highly complicated piece of machinery. In the opinion of the author it is inclined to be over-elaborate, the pulley system giving sufficient accuracy, and moreover being much less expensive than a precision screw assembly.

The whole spectrometer is supported upon a heavy channel base which can be levelled by means of six heavy screws. The main collimator A and detector head D are placed beyond the curved crystal on an elevated base, and will be fully described in sections (IV) and (V) of this chapter.

The wavelengths to be measured by the spectrometer are proportional the sine of the angle θ at which the radiation is incident on the transverse planes of the crystal. From figure (4) it can be seen that triangle CR'B is a right triangle with constant hypotenuse CR'. Thus the wavelength of the incident radiation is proportional merely to the length of the leg R'B of this triangle. This length corresponds to

the distance of travel of the spur gear along the rack from the "zero" position, and is measured by means of the brass disc geared to the rack and pinion assembly. The disc can be read to one two-hundreth of a revolution on a scale around its circumference, the total number of complete revolutions being determined by a small revolution counter fixed to its axle. This measurement can then be translated into wavelength units with the aid of a simple arithmetic calculation.

(II) SOURCE AND SOURCE MOUNT DESIGN

Source Design

To date, two sources of Iridium-192 have been used in the spectrometer. The source holder design was different for each of the sources.

The first source consisted of a rectangular piece of iridium foil, 0.125 in. wide, 1.12 in. long, 0.002 in. thick, and 142 mg. in weight. As a precaution against radiation hazards the source holder was doubly sealed. Figure (6) shows the elements of this source container. The iridium foil was first sheathed in a thin-walled aluminum cylinder with one end open. The sheath was then squeezed tightly around the foil, and the open end clamped over to form a seal. Since this part of the source holder was to be irradiated in the neutron flux from an atomic pile along with the iridium, the aluminum was of a necessarily high purity. The impurities present in the aluminum were as follows: Fe - 0.002%, Cu - 0.002%, Mg - 0.001%, Si - 0.001%,

Mn and Ni - 0.001%. Upon removal from the pile the sheathed ribbon A was inserted into a radial slot B running parallel to the axis of a mild steel cylinder C. One end of this cylinder was closed by a thin aluminum disc D fastened with a screw S'. This disc carried a slot S. The whole was then slid into a close-fitting thin-walled aluminum cylinder C' closed at one end.

The second source was designed to facilitate the handling of the source when it was removed from the pile. Once again the source consisted of a rectangular piece of iridium foil, 0.007 in. wide, 1.4 in. long, 0.004 in. thick, and 17.5 mg. in weight. This time, however, it was inserted in a radial slot running parallel to the axis of a high-purity aluminum cylinder. This slot was closed by "ploughing" the aluminum over the top of the foil, and the cylinder placed in a thin-walled aluminum shell whose ends were forced over the cylinder, thus supplying a double seal. The entire assembly was irradiated in the pile, and upon removal a mild steel bolt was inserted in an aperture running the entire length of the centre of the aluminum cylinder. The bolt, which was tightly screwed into the aperture, carried an allen-head slot at the upper end.

In each case the source container was mounted in the spectrometer in such a way that the source had its long axis vertical and its flat faces parallel to the direction of gamma-ray propagation from source to crystal. In such a position the source itself acts as a spectroscopic slit.

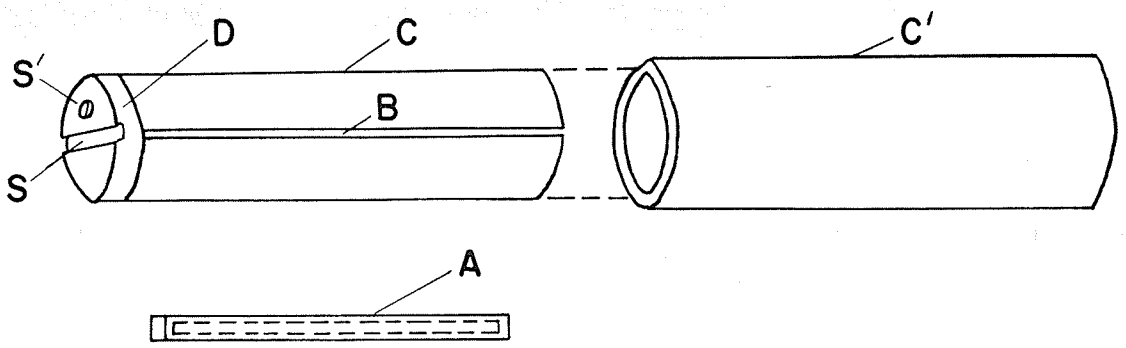

FIG 6 SOURCE CAPSULE

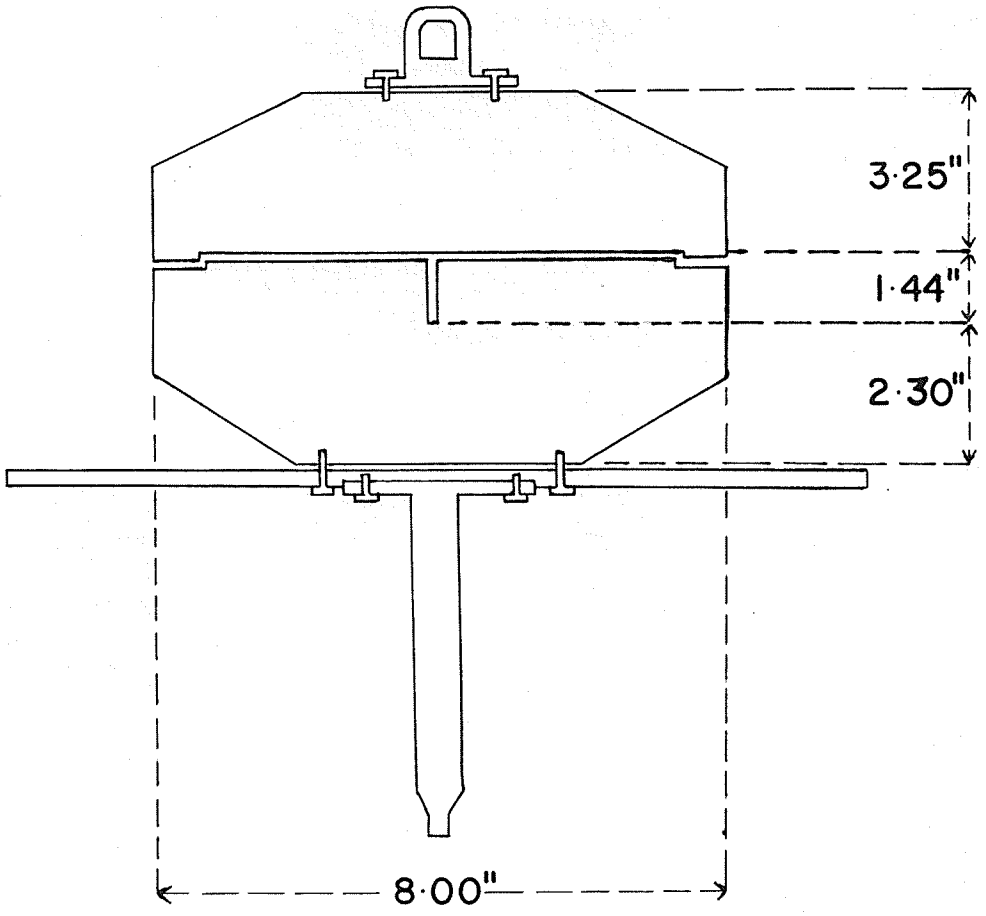

FIG. 7 SOURCE MOUNT

Source Castle

The source castle shown in figure (7) is in the form of a bevelled cylinder machined from two cast pieces of a lead-tin-antimony alloy. Figure (7) is a vertical section through the castle. The source mount, which has a radius of 4 in., is designed to give maximum protection from the intense source without overloading the upper radial beam. The lower section of the castle has a cylindrical well, 1.44 in. deep and 0.203 in. in radius, drilled out to accommodate the source capsule. Leading out from the well is a narrow tapering channel which allows the radiation from the source to impinge upon the curved crystal. Securely bolted to the bottom of the lower section of the castle is a steel plate carrying a cylindrical steel axle, the tip of which is bolted to the centre of a ball race assembly on the end of the radius bar. This section of the castle is very precisely machined to allow the positioning of the leading edge of the source directly above the centre of the bearing on the radius bar. The upper section of the castle rests on the lower section in such a way that their edges overlap as a precaution against radiation hazards. It is fitted with a large steel eye to accommodate the hook from a remote control crane.

Source Mounting Technique

Due to the high strength of the sources needed, a remote control technique had to be evolved for mounting the source container. The mild steel sections of the source capsule were designed for use in this mounting procedure.

A small electromagnet was designed for carrying the source at the end of a long rod. Figure (8a) shows the cross-section of the electromagnet which is in the form of a cylindrical steel case of radius 1.125 in. bolted to a central steel core 0.375 in. in radius. After machining, the steel was heated to white heat and allowed to cool slowly to ensure that the assembly would not retain any permanent magnetism. Around the core is wound approximately six hundred turns of insulated copper wire having a total resistance of 1.2 ohms. A suitably strong field can be developed at the pole of this magnet using a 2.0 volt battery supply, only 2.5 watts being dissipated in the coils.

The complete assembly of electromagnet and rod is shown in figure (8b). Screwed into the central core of the electromagnet is a 9 in. length of cylindrical aluminum stock which passes through the end of a hollow cylindrical tube and is fitted with a horizontal pulley. Two parallel belts of steel piano wire link this pulley with another horizontal pulley at the other end of the tube. Thus, by turning the second pulley the operator can rotate the electromagnet through 360°. The wire connections from the electromagnet pass through the hollow tube and are attached to a 2.0 volt battery. A switch is located on the tube so that, by merely depressing a button, the operator can cause the electromagnet to function.

When mounting the source, the operator of the electromagnet is always in the shadow of a large lead shield,

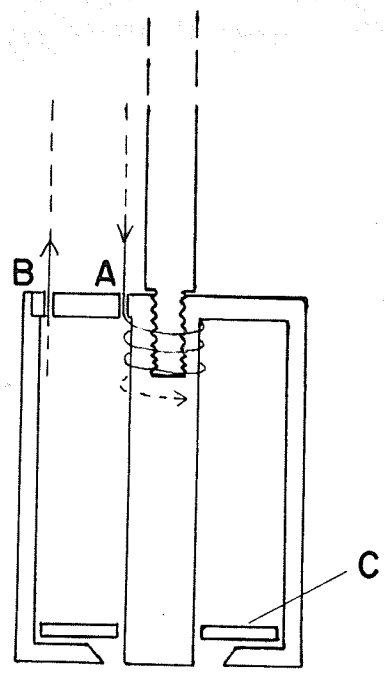

A - ENTRY POINT OF WIRE
B - EXIT POINT OF WIRE
C - INSULATED WASHER

(a) ELECTROMAGNET

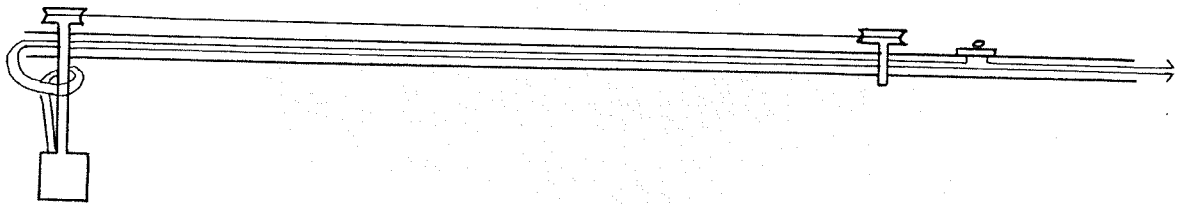

(b) COMPLETE UNIT

FIG. 8 REMOTE CONTROL ASSEMBLY

the source being viewed by means of a suitably placed periscope. After insertion in the source castle well, the source may be oriented by rotating it with a screwdriver attachment which can be fitted to the base of the electromagnet. The top of the lead castle is now lowered over the source using a remote control crane.

(III) CRYSTAL CLAMPING ARRANGEMENT

The diffracting crystal used in the spectrometer is a thin rectangular lamina of quartz 0.040 in. thick. The flat faces of the crystal slab are accurately parallel and polished optically flat. The transverse reflecting planes used in this case were the (310) planes which have a grating distance of 1.175A°. Before bending, it is of the utmost importance to remove any incipient cracks in the surfaces and edges of the slab. This was done by immersing the crystal in hydrofluoric acid, the edges of the slab being etched for a much longer time than the surfaces which were immersed just long enough to remove the detritus left behind from the grinding and polishing processes. To ensure that all the incipient cracks had been removed the crystal was carefully examined under a high power microscope.

To bend the crystal to the correct curvature, the slab was compressed between two tempered blocks of stainless steel, one of which has a convex cylindrical profile, and the other a concave cylindrical profile. The method of precision profiling these blocks has been fully described by

Dumond[6]. The curvature of the crystal is determined only by the curvature of the convex block since a rubber gasket separates the crystal slab from the concave block. The two blocks are held together by four bolts fitted with helical springs. Pressure is applied by springs rather than by the bolts directly, to allow for any small contractions or expansions due to temperature changes. The convex block has a ribbed window of dimensions 2.25 in. by 1.88 in. to allow the radiation to impinge upon the crystal. The purpose of the ribs is to supply the centre of the crystal with support and to ensure an accurately curved profile. Before compressing the crystal, the inner surfaces of the clamping blocks were thoroughly cleaned with carbon tetrachloride to remove any particles of dust or grease which might radically change the radius of curvature.

When the crystal has been inserted, the blocks are clamped to a steel table attached to the top of the vertical shaft, about which the upper and lower radial beams are free to pivot, in such a position that a vertical line through the centre of the crystal coincides with a line through the centre of the shaft. The means of clamping is provided by two L-shaped pieces of steel bolted to the table. The table itself has a machined horizontal top and may be rotated in a horizontal plane about the shaft.

To ensure that the (310) planes in the quartz slab were accurately vertical, a technique had to be devised for rotating the crystal in a vertical plane. As shown in

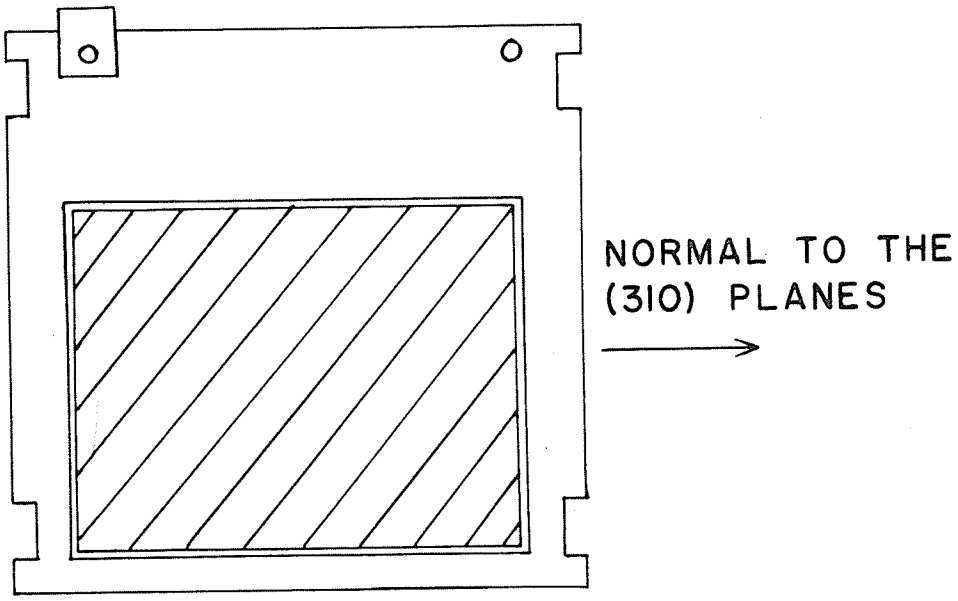

FIG. 9 QUARTZ CRYSTAL WITH ENCLOSING TEMPLATE

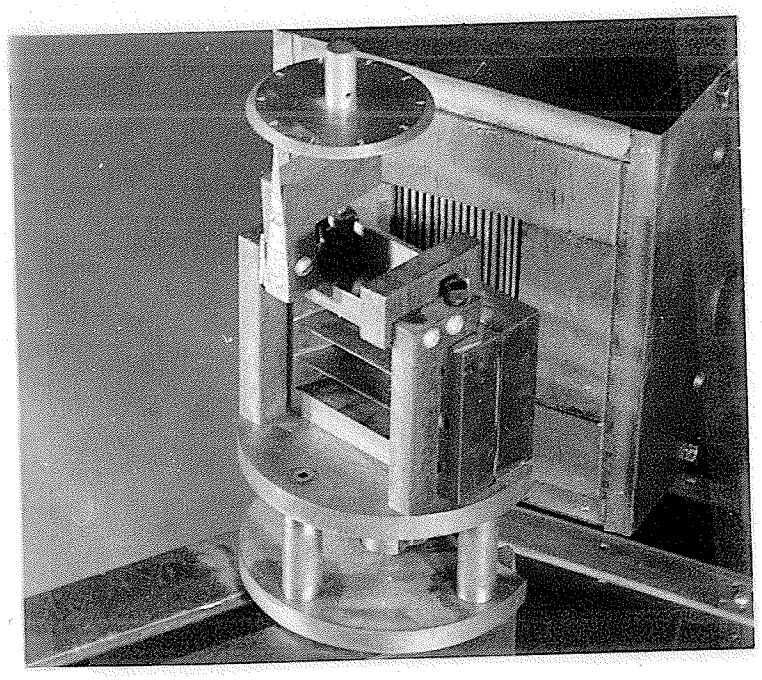

PLATE. 2 CRYSTAL CLAMPING ASSEMBLY

figure (9) the crystal is supported in an aluminum template 0.03 in. thick, one corner of which is fitted with a small cylindrical steel anvil. Plate (2) shows the crystal and blocks in actual position on top of the table. The upper edge of the template protudes above the top of the clamping blocks. The corner of the template opposite to the one carrying the anvil fits into a slot in the head of one of the L-shaped clamps, where it is pivoted by means of a cylindrical brass plug passing through the template and into the clamp. The template, and consequently the crystal, can thus be rotated in a vertical plane about this point by applying pressure on the anvil. Pressure is applied to the anvil by a fine-thread screw passing down through the head of the L-shaped clamp. This screw ends in a spherical tip and is fitted at its upper end with a cylindrical brass disc which can be read to one two-hundreth of a revolution. Any backlash is removed from the assembly by a small spring linking the corner of the template to the head of the L-clamp.

(IV) COLLIMATOR

Since the Bragg angle of reflection is very small for high energy gamma-rays, the low wavelength region of the selectively reflected spectrum is masked by the intense direct beam of radiation which passes undeflected through the curved crystal. To shield the detector from this intense direct beam of scattered gamma-rays a system of lead fins, or baffles, is interposed between the curved crystal and the detector.

The baffle system, designed to have a theoretical transmission of 50%, is enclosed in a rectangular steel casing, the walls of which are lined with solid lead. Figure (10) is a perspective line drawing of the entire assembly with the upper steel wall and lead liner removed from the casing to reveal the system of baffles. The casing, of outer dimensions 30.0 in. x 6.9 in. x 7.9 in. is constructed of rigid steel plates, 0.625 in. thick, securely bolted together. Bolted to the upper and lower walls, and running the full length of the casing, are two rectangular blocks of lead 1.56 in. thick. Bolted to the side walls are two trapezoidal blocks of lead, 1.625 in. thick at the entry end of the channel and 0.982 in. thick at the exit end. Thus, a tapering channel is provided for the diverging reflected beam of radiation.

The system of baffles which fits snugly into the casing is constructed of seventeen narrow fins cast from a lead-tin-antimony alloy. Great care was taken in the casting of these fins to ensure that they contained no air bubbles and were not warped in any way. The effect of warped fins will be discussed in a later section. These alloy fins, 30.0 in. long and 0.0625 in. thick, are separated by brass spacers clamped at several positions along the top and bottom of the fins in such a way as to produce eighteen tapering channels each 30.0 in. long, 3.50 in. high, 0.0625 in. wide at their entry ends, and 0.134 in. wide at their exit ends.

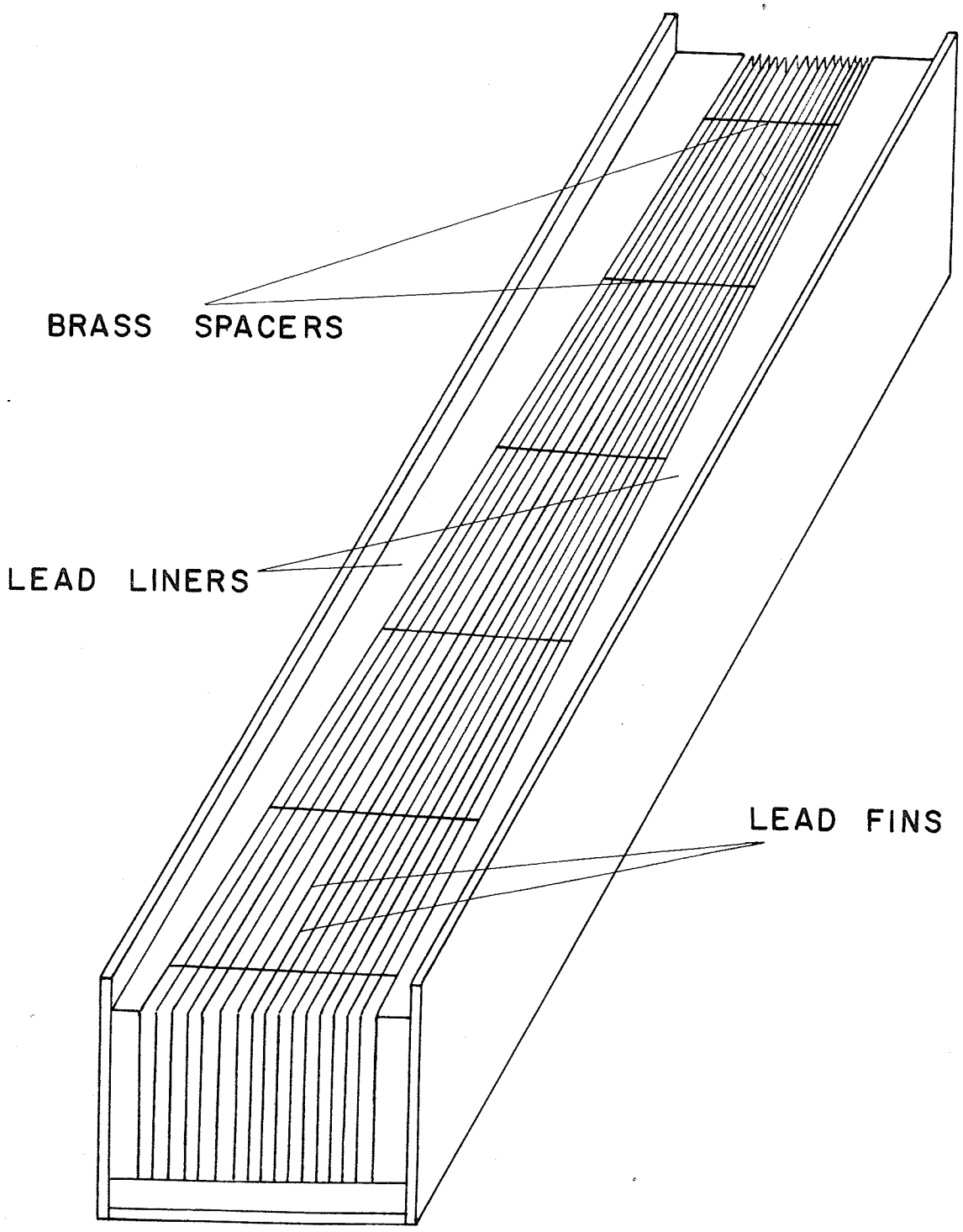

FIG. 10 PERSPECTIVE LINE DRAWING OF THE MAIN COLLIMATOR

It is now obvious that if the collimator is aligned such that planes through the centres of each channel intersect in a vertical line through the virtual image point V [figure (4)], theoretically 50% of the selectively diffracted beam will reach the detector, while the major part of the direct beam will be absorbed.

(V) DETECTOR SYSTEM

The system used to detect the selectively reflected gamma-rays is essentially a scintillation spectrometer operated in tandem with the curved crystal spectrometer.

The radiation is detected in a thallium-activated sodium iodide crystal grown by the Harshaw Chemical Company, Cleveland, Ohio. The crystal, which is in the form of a cylinder 5.50 in. in diameter and 3.0 in. thick, is enclosed in a thin aluminum container with a glass face for viewing the scintillations produced by the gamma-rays. The scintillating crystal is mounted on the end of the main collimator so that it intercepts the gamma-ray beam reflected from the curved crystal. The scintillations produced in the crystal are converted into electron pulses by a 5.0 in. DuMont photomultiplier tube type 6364. Optical contact is provided between the face of the photomultiplier tube and the scintillating crystal by Dow-Corning silicone fluid of viscosity 10^6 centistokes.

Figure (11) is a vertical section through the complete detector assembly. The mounted crystal A is held

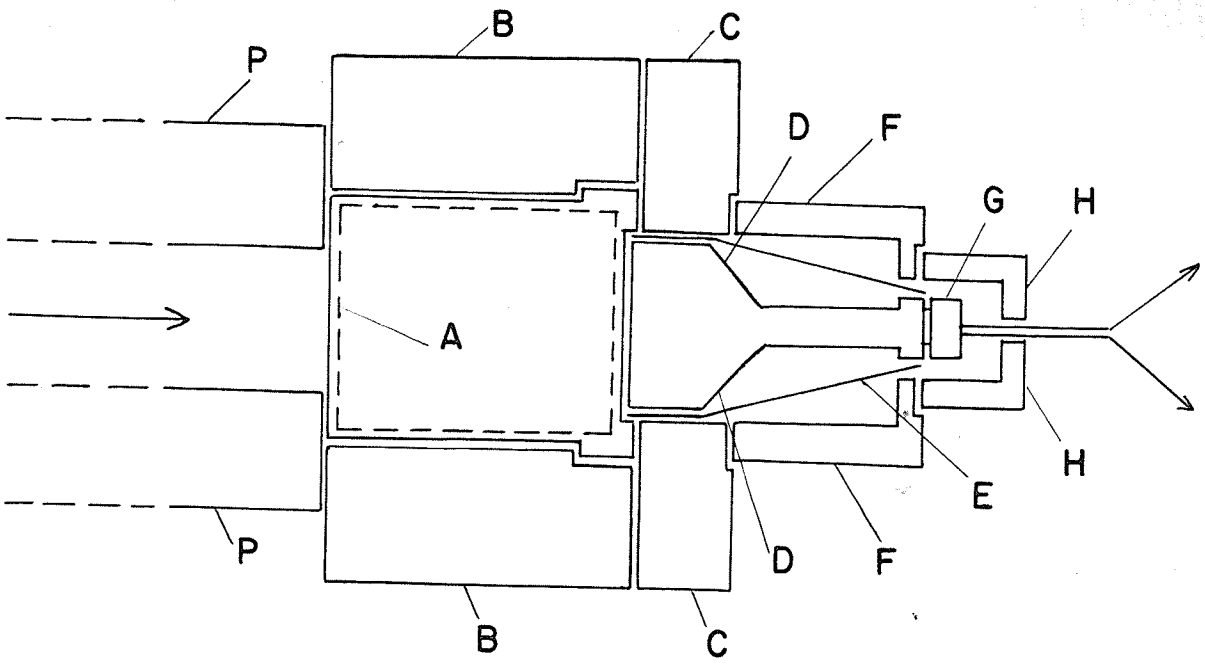

FIG. 11 DETECTOR HEAD ASSEMBLY

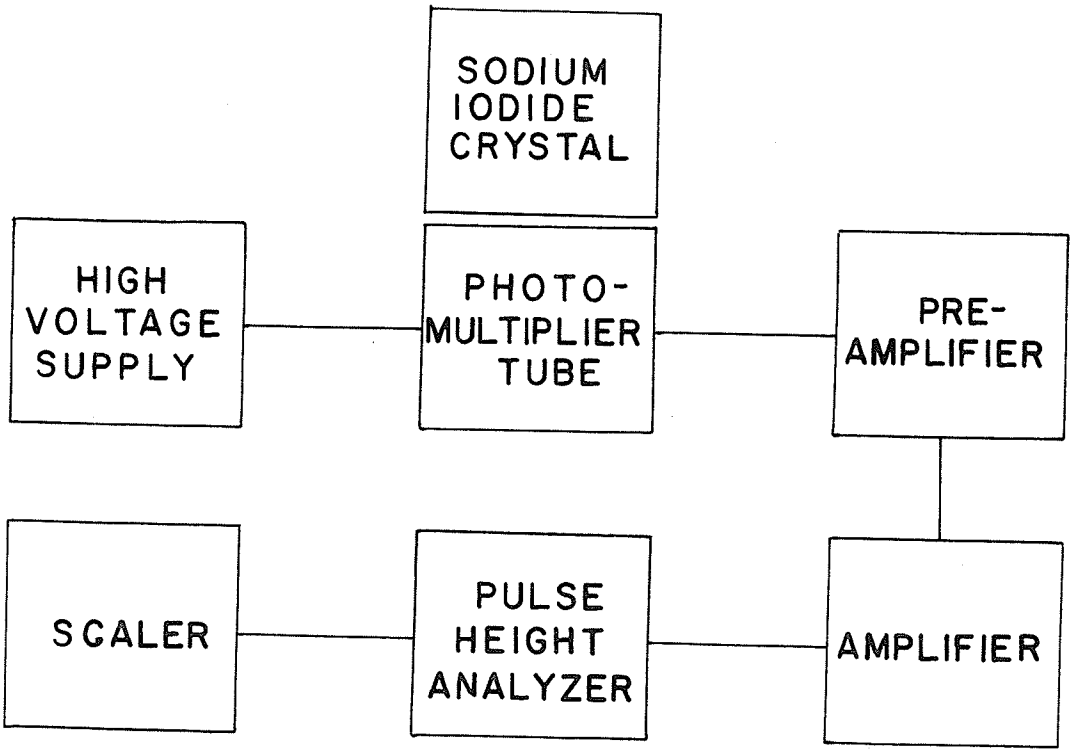

FIG. 12 BLOCK DIAGRAM OF THE SCINTILLATION SPECTROMETER

tightly against the collimator P by means of an anular lead cylinder B, 2.5 in. thick and 4.5 in. long, bolted to the steel walls of the collimator. A further anular lead cylinder C, 3.0 in. thick and 2.5 in. long, holds the crystal securely within the first lead cylinder and also provides a seat for the photomultiplier tube D. The photomultiplier tube is enclosed in a thin magnetic shield E, and is shielded from stray radiation by a lead cylinder F which has a wall thickness of 1.0 in. and has one end closed except for a small aperture to accommodate the stem of the photomultiplier tube. The base G of the photomultiplier tube is a normal cathode follower type base designed for use with a positive high voltage. It is also enclosed in a small lead cylinder H with a wall thickness of 1.0 in. and an aperture for the high voltage input lead and the output signal lead. Not shown in figure (11) are two massive blocks of lead strapped to the side walls of the collimator directly in front of the anular cylinder B. These blocks protect the crystal from the intense direct beam of radiation when the source is far out from the "zero" position. All the joints on the detector assembly are masked with electrical tape to ensure a good light-tight seal.

Figure (12) is a block diagram of the entire scintillation spectrometer. A positive high voltage of the order of 1000 volts is applied to the base of the photo-multiplier tube. The resulting electron pulses are fed into a preamplifier with a variable gain of 1, 5, or 10, and then into a non-overload linear amplifier which has a range of

gains up to 7000. Both the model 359 preamplifier and the model 358 amplifier are products of Franklin Electronics Inc., Bridgeport, Pennsylvania. The amplifier is equipped with a pulse height analyzer unit. This unit selects pulses which fall within variable upper and lower discriminator voltage levels, and passes them on to a decade scaler, type SG-3A, built by Technical Measurement Corporation, Newhaven, Connecticut. 110 volts A.C. is supplied to the units of the scintillation spectrometer by a 60-cycle voltage regulator, model 3000S, built by Sorenson and Company, Stamford, Connecticut. For convenience, all units except the pre-amplifier are mounted in a dexion rack at one side of the curved crystal spectrometer. The preamplifier, which must necessarily be close to the signal source, is mounted on top of the lead detector assembly.

Chapter 3 - Alignment of Spectrometer

(I) PRELIMINARY MECHANICAL ALIGNMENT

Test for Rack Uniformity:

For the spectrometer to be useful for the precision determination of gamma-ray energies it is of the utmost importance that the wavelength scale of the instrument be linear. Since the wavelength measurements in the spectrometer under consideration are directly proportional to the distance of travel along the rack described in chapter 2, section II, it was essential to determine as early as possible whether there were any readily apparent non-linearities in this rack. An optical system was devised to do this.

A small front-surface plane mirror was mounted on top of the vertical shaft, about which the upper and lower radial beams rotate, in such a way that the plane face of the mirror was vertical and normal to the upper radial beam. A light source was set up at one side of the radial beam, and a slit and lens placed so that parallel light fell on the mirror. The image of the slit was reflected into a 6 in. front-surface spherical mirror, of focal length 5.0 feet, on the opposite side of the radial beam. The image from spherical mirror was then located at the centre of the cross-hairs of a horizontal travelling telescope placed approximately at the focal point of the spherical mirror. The upper radial beam was now rotated by the rack and pinion system, and the image located in the telescope for each individual setting of the driving mechanism. For simplicity, the image

of the slit was located after each complete revolution of the brass driving disc.

Since the spur gear has 12 teeth and a pitch of 20, one revolution of the brass driving disc corresponds to a distance along the rack of:

$$dx = \frac{1}{50} \cdot \frac{12}{20} \cdot \pi \text{ in}$$

$$= 0.0377 \text{ in}$$

Consider figure (4) for a moment. If x is the distance along the rack from the "zero" position, and A is the constant distance CR',

$$\text{then } \sin \theta = x/A$$

Consequently, a small increase dx in x will cause a small change in the angle of the upper radial beam:

$$d\theta = \frac{A\, dx}{(A^2 - x^2)^{1/2}}$$

This in turn will cause the image of the slit to turn through an angle of 2 $d\theta$. Thus, the transverse horizontal distance moved by the telescope when x goes to $x + dx$ is proportional to

$$\frac{dx}{(\text{const.} - x^2)^{1/2}}$$

If the rack is uniform, therefore, the distance travelled by the telescope per revolution of the brass disc should be constant over a small region of the rack, and should increase slightly as the outer regions of the rack are investigated. The fact that the telescope travels in a straight line rather than on the arc of a circle will have a negligible effect.

Consider figure (13). Graphs (a), (b), and (c) are plots of the distance travelled by the telescope versus the distance of travel along the rack. Graph (a) is a typical example of the results first obtained. It showed violent discontinuities and wide variations from the mean distance travelled by the telescope. The rack and spur gear were examined under a powerful lens, and several of the teeth were seen to have protuding burrs. These were very carefully, removed with a file and fine emergy cloth, and any particles of dirt or metal chips cleaned from the teeth. The rack was then lightly oiled and covered with an aluminum hood to protect it from dust. The tension in the spring for removing backlash was slightly increased. Graph (b) was obtained for the same portion of the rack after the adjustments had been made. No discontinuities were now apparent. Graph (c) is a typical example of the results obtained for the outer regions of the rack.

A review of all the results revealed no obvious non-uniformities in the rack, all the graphs being straight lines within the limits of the observational errors. An extensive search for any possible periodicity in the behaviour of the rack and pinion assembly produced negative results. It must be remembered, however, that in this case the linearity of the rack was compared only with the linearity of the transverse vernier scale on the telescope. This vernier scale was assumed to be of sufficient accuracy to reveal any obvious defect in the rack. A more precise determination of the rack behaviour will be discussed in a later section.

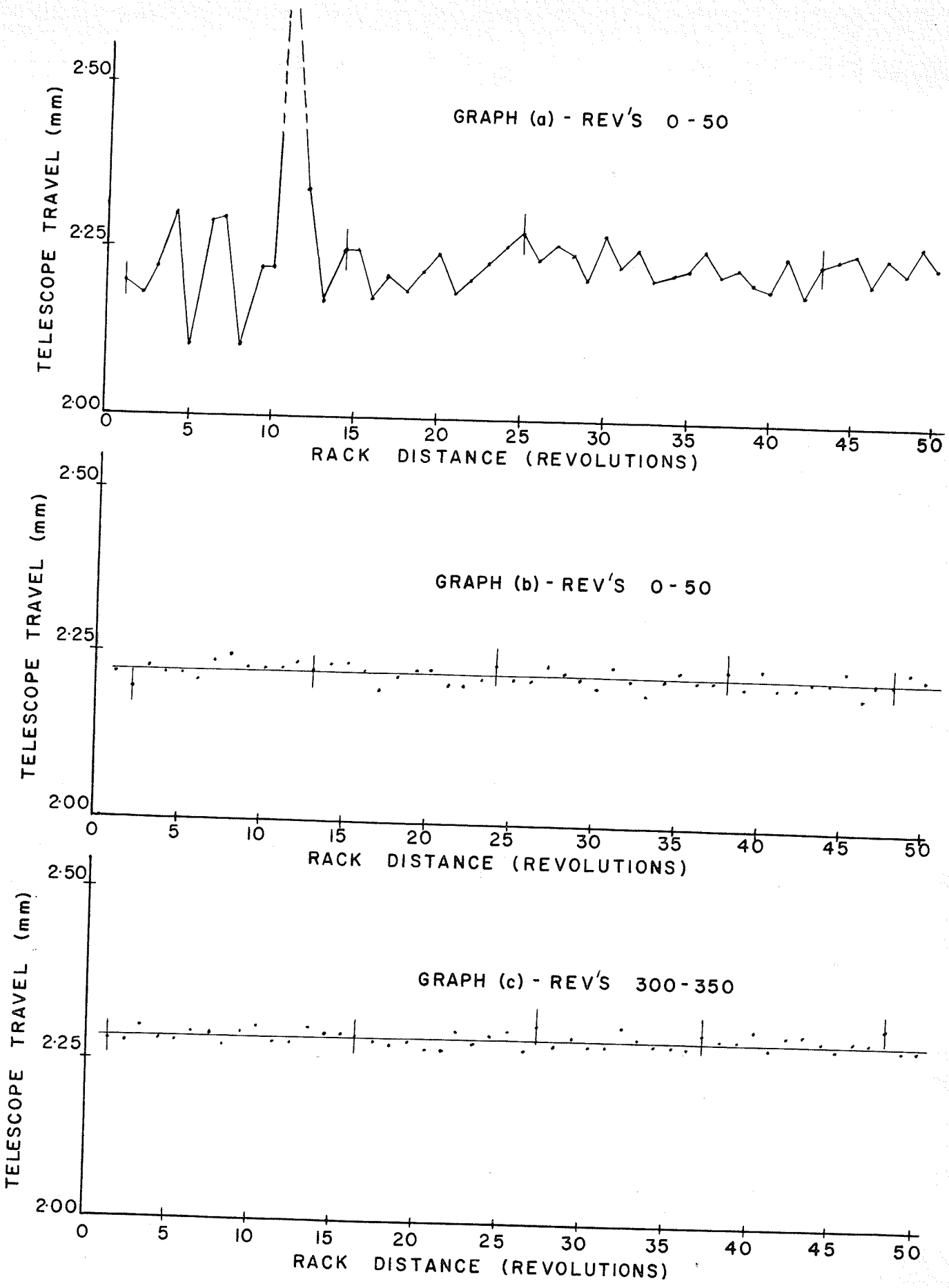

FIG.13 RACK CHARACTERISTICS

Radius of the Crystal Clamping Blocks:

The exact radius of curvature of the crystal clamping blocks must be known before the spectrometer can be correctly aligned. It is also of great interest to know whether the crystal clamping blocks have the same radius over the entire working aperture.

A piece of silvered glass was mounted in the clamping blocks in exactly the same manner as the quartz crystal was to be mounted. The blocks were securely mounted on one end of an optical bench so that the aperture of the crystal pointed down the length of the bench. Mounted on the other end of the optical bench was a metal screen with a narrow vertical slit, and behind it an intense light source. The image of the slit was reflected by the curved mirror and located back on the screen just to one side of the physical slit. The screen was then moved along the bench until the image of the slit was sharply in focus as determined by a strong lens. The distance from the centre of the crystal aperture to this point was then carefully measured, this distance being in fact the radius of curvature of the clamping blocks.

Several independent measurements were made to determine the radius with the greatest possible accuracy. The blocks were taken apart several times, cleaned, and reassembled to insure that particles of dirt introduced no spurious results. Tests were run,both with the clamping bolts tightly screwed down, and again with the helical springs applying most of the pressure, to determine whether or not

the springs were functioning correctly. Tests were also run with half of the aperture vertically blocked off in an attempt to find any change in the radius of the aperture from one side to the other.

The results are listed in tables (1a) and (1b). The helical springs were found to apply sufficient pressure, no difference in the radius of curvature being discerned when the clamps were bolted with or without the springs. The attempt to see any change in the radius of curvature of the aperture from one side to the other proved futile since focusing the image of the slit was much more difficult when only one side of the aperture was used.

The value for the radius of curvature of the crystal clamping blocks was taken as 124.20 ± .05 cm.

Table (1a): Radius of the clamping blocks with the bolts screwed tightly down

	Radius (cm)		
	Full Aperture	Half Aperture	Half Aperture
	124.24 ± .05	124.0 ± .2	124.4 ± .2
	124.16	124.2	124.1
	124.22	123.8	124.2
	Blocks Reassembled		
	124.20	124.6	124.0
	124.22	124.3	124.0
	124.18	124.2	124.1
	Blocks Reassembled		
	124.18	124.2	124.3
	124.16	124.2	124.5
	124.22	123.9	124.2
Mean	124.20	124.2	124.2

Table (1b): Radius of the clamping blocks using the helical springs

Radius (cm)		
Full Aperture	Half Aperture	Half Aperture
124.19 ± .05	124.3 ± .2	124.5 ± .2
124.20	124.2	124.1
124.24	124.5	124.2
Blocks Reassembled		
124.23	123.8	124.2
124.23	124.5	123.9
124.19	124.1	124.4
Blocks Reassembled		
124.18	124.5	124.2
124.17	124.0	124.3
124.17	124.2	123.9
Mean 124.20	124.2	124.2

Spindle Alignment:

Due to the highly complicated mechanical features of the spectrometer, great pains had to be taken to ensure the correct alignment of the various spindles employed in the machine. It was also necessary to set up the mechanical "zero" of the spectrometer.

The first task was to find the position in which the track T was perpendicular to a line through the centres of the main spindle B', about which the track T pivots, and the vertical shaft about which the upper and lower radial beams rotate. This position is in fact the "zero" position of the wavelength scale. Consider figure (14a). r_1 and r_2 are portions of the parallel cylindrical steel rails of the track T. The bearing B', on which the track rotates, is linked with the track by a bolt passing up through the base plate of the track into a small cylindrical boss B_1'. The centre of this boss is vertically above the centre of the bearing B'. K is the cylindrical housing through which the vertical shaft supporting the curved crystal passes. Its centre G thus lies on the axis of spindles C_1 and C_2 [see figure (5)] . The distance B'E was measured as accurately as possible and a vertical line passing through D' set up so that the distances B'E and D'E' were rigorously equal. This vertical line was physically realized using two machinist's squares mounted on the rails r_1 and r_2 as shown in figure (14b). B'D' thus represents a straight line running parallel to the track runners and passing through a point in space vertically above the centre of the track bearing. The

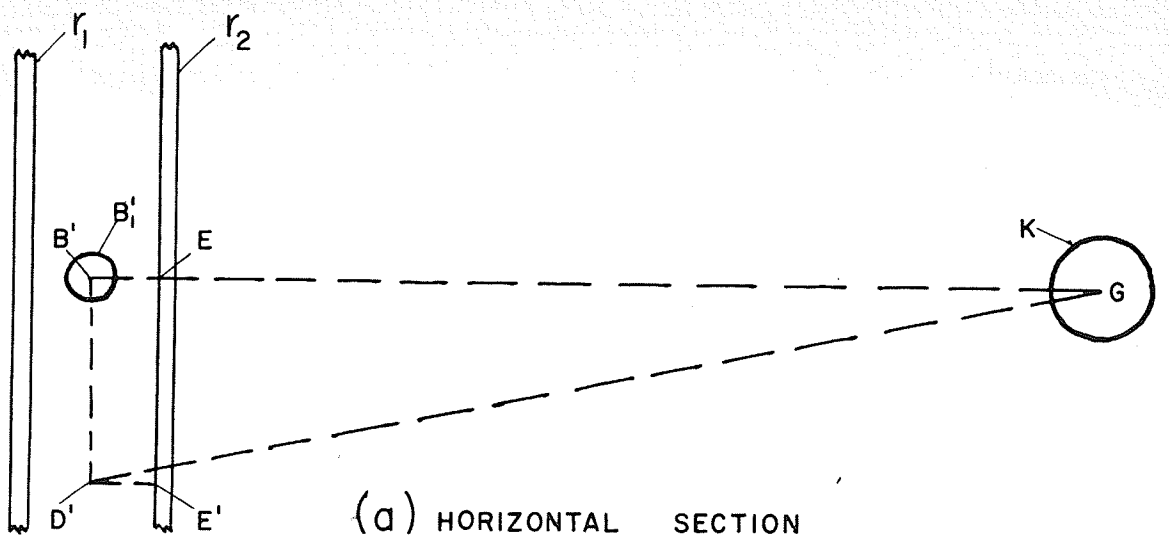

(a) HORIZONTAL SECTION

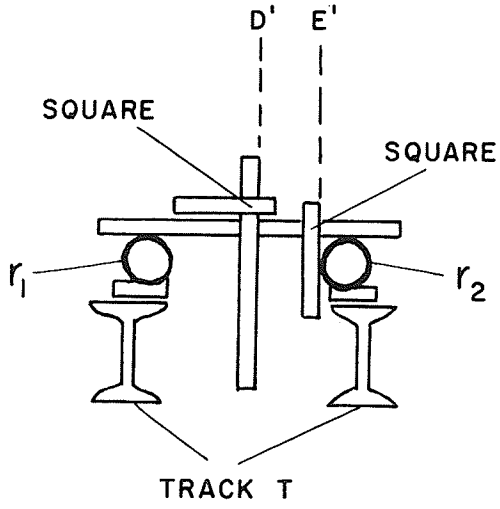

(b) VERTICAL SECTION

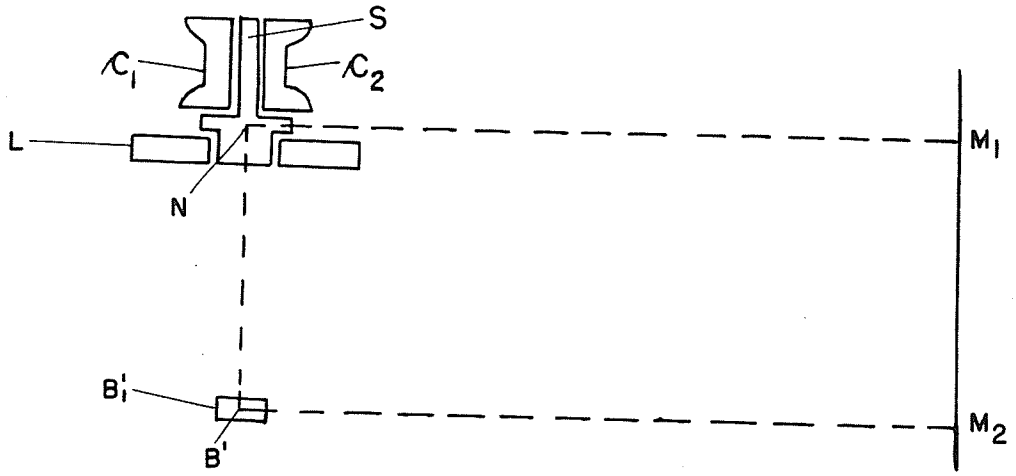

(C) VERTICAL SECTION

FIG. 14 SPINDLE ALIGNMENT

problem was to find the position of the track such that the line B'G was perpendicular to the track. If the track is in this position, D'G should be the hypotensue of the right triangle B'D'G. The distances B'G, B'D', and D'G were accurately measured. Care was taken to ensure that these measurements were in a horizontal plane. The measured value of D'G was compared with the calculated value of the hypotenuse of a right triangle having its other sides of length B'G and B'D . The track was then rotated until these two values were equal within the limits of the observational error of ± 0.05 cm. To ensure the best possible accuracy, the measurements were repeated with D' at several different positions on either side of B'.

A similar procedure was followed to ensure that the cylindrical steel shaft terminating the lower radial beam II was at right angles to the track. This time, however, the two sides of the right triangle opposite to the hypotenuse were physically realized by the steel shaft itself and the rail r_1 of the track T.

The centre of the end of the upper radial beam I had now to be located vertically above the centre of the track bearing B'. This end of the beam rests on a small carriage L [see figure (4)]. Consider figure (14c). B_1' is a vertical section through the cylindrical boss shown also as B_1' in figure (14a). The carriage L is fitted with a vertical steel shaft S which passes up through the centre of the channel sections c_1 and c_2 of the upper radial beam I. A

vertical line M_1M_2 was set up about one meter to the side of the spectrometer so that it was in a vertical plane through the centre of, and parallel to, the track rails. This line was physically realized by one edge of a machined steel plate which was blocked into a vertical position. The horizontal distances NM_1 and $B'M_2$ were carefully measured. The carriage L was now unclamped from the piano wire of the pulley assembly, and moved until NM_1 and $B'M_2$ were equal. At this point the carriage was securely linked to the pulley assembly once again. The centre of the upper radial beam was thus positioned vertically above the centre of the track bearing to within $\pm$ 0.05 cm.

With the driving mechanism disassembled, the brass disc and revolution counter were set at some arbitrary value, this value being in fact the theoretical "zero" of the wavelength scale. The driving assembly was then rigidly connected to the track again.

As seen in figure (4b), when the spectrometer is in the "zero" position, the centre of the source carriage R, and consequently the leading edge of the source, the centre of spindle O linking the radius bar to the lower radial beam, and the centre C of the vertical shaft, about which the radial beams rotate, must lie in the same vertical plane. This was approximately realized by setting up a long brass rod along the length of the spectrometer so that the distances to the edge of the rod from the axis of spindle C_1 and C_2 and from the centre of the bearing linking the source carriage to radius bar I were equal. The centre of spindle O

was then positioned at exactly the same distance from the edge of the rod and spindle O securely bolted to the lower radial beam II to prevent any transverse motion. It was still free, however, to move in a longitudinal direction along the length of the radial beam. It was now located as accurately as possible in such a position that the distance between its centre and the axis of spindles C_1 and C_2 was half the radius of curvature of the crystal clamping blocks, i.e. 62.10 cm. Spindle O was then bolted securely to prevent longitudinal motion and the length of the radius bar I also adjusted to 62.10 cm., thus locating the leading edge of the source at the centre of curvature of the quartz crystal. Due to the difficulty in making accurate measurements, the centre of the spindle could be positioned on the radial beam only to within $\pm$ 0.2 cm. in both longitudinal and transverse directions. The final adjustment of this spindle had to wait until the spectrometer was in actual operation.

Although not a direct part of the spindle alignment, two other mechanical adjustments will be described in this section. Firstly, the spectrometer was levelled as accurately as possible, particular care being taken to ensure that the track T and carriage Q were horizontal. Any departure from the horizontal in the track or carriage will cause a corresponding departure from the vertical in the long axis of the source. This will produce a considerably thickening of the line source viewed by the crystal and must be avoided at all costs. A 15 in. Lufkin Master Precision Level was used to level the carriage and the track. This instrument was capable of detecting a drop of less than 0.0005 in. in one

foot. The entire lengths of the carriage and the track were investigated, any departures from the horizontal being removed by the use of thin shims. The main collimator was also levelled in both longitudinal and transverse directions using this precision level. In this case the levelling was accomplished by means of three levelling screws upon which the collimator rests. Finally, to ensure that the radiation beam reflected from the curved crystal was horizontal, the source carriage was raised by means of shims until the centre of the source aperture was at exactly the same vertical height as the centre of the working aperture of the crystal.

Collimator Alignment:

The main collimator rests on three heavy levelling screws on an elevated portion of the base of the spectrometer. The two screws supporting the entry end of the collimator rest on a narrow steel bar which fits snugly into a transverse groove in the top of the base. The ends of this bar are L-shaped and protude about one inch on either side of the base. Bolts are screwed through each L-shaped end and contact the side of the base. The bar, and consequently the end of the collimator, can thus be moved in a transverse direction across the top of the base by turning one of the bolts. The levelling screw supporting the exit end of the collimator fits into a groove in an exactly similar bar, thus allowing the exit end of the collimator to be aligned.

The entrance aperture of the collimator must be aligned so that its centre is collinear with the centre of the source aperture and the centre of the working aperture of the crystal when the spectrometer is in its "zero" position.

A long rigid steel rod was mounted such that it passed through the centre of the source aperture and over the centre of the table mount on the vertical shaft about which the radial beam rotate. The entry end of the collimator was then adjusted until the distances measured from either side of the collimator to the centre of the rod were equal.

The exit end of the collimator is in correct alignment only when the narrow tapering channels converge to a vertical line at the leading edge of the source. With the curved crystal removed, a 20 millicurie radioactive source of Zn-65 was mounted on the source castle in such a position that its centre was located as near as possible to the centre of the source aperture. This relatively weak source was used instead of the strong source of Ir-192, designed to fit snugly into the source aperture, since its weak radioactivity would not saturate the scaler when the spectrometer was positioned so that the intense beam of radiation passed directly down the collimator and into the scintillating crystal. The upper radial beam was now driven along the track on either side of the "zero" position, the intensity of the transmitted beam being measured on the scaler for each individual setting of the driving mechanism. In this case, the pulses coming from the amplifier were passed into the scaler not from the differential output of the pulse height analyser but from the integral output. Thus, except for the increased efficiency of the scintillating crystal, the scintillation spectrometer was operated essentially as a geiger counter. If a graph of counting rate versus source

position is drawn it will obviously consist of a sharply rising peak, the top of which will occur when the source is at the line of intersection of the collimator channels. For the collimator to be correctly aligned, therefore, this peak must be symmetrically situated about the previously determined mechanical "zero". The exit end of the collimator was moved transversely across the base of the spectrometer until this situation was reached. The collimator was then fully aligned.

Figure (15) is a graph of counting rate versus source position. For convenience, the source position is plotted in terms of the number of revolutions of the brass driving disc. The dotted lines indicate the ideal transmission characteristic for the collimator if there is no scattering by the lead partitions. Note that the peak has a slightly flattened top. This has the advantage over a sharp peak in that the intensity readings on the spectrometer will be slightly less sensitive to a misalignment of the collimator relative to the reflected beam. The sharply rising nature of this peak makes it clear that the spectrometer cannot be effectively used within 6 revolutions of the brass disc on either side of the "zero" position. Now 6 revolutions of this disc out from the "zero" position corresponds to a wavelength setting of

$$\lambda = \frac{2\,d \sin\theta}{n}$$

$$= \frac{2 \times 1.175 \times 6 \times 0.0377}{52.00}\ A^{\circ} \text{ for 1st order reflections}$$

$$= 10.22\ MA^{\circ}$$

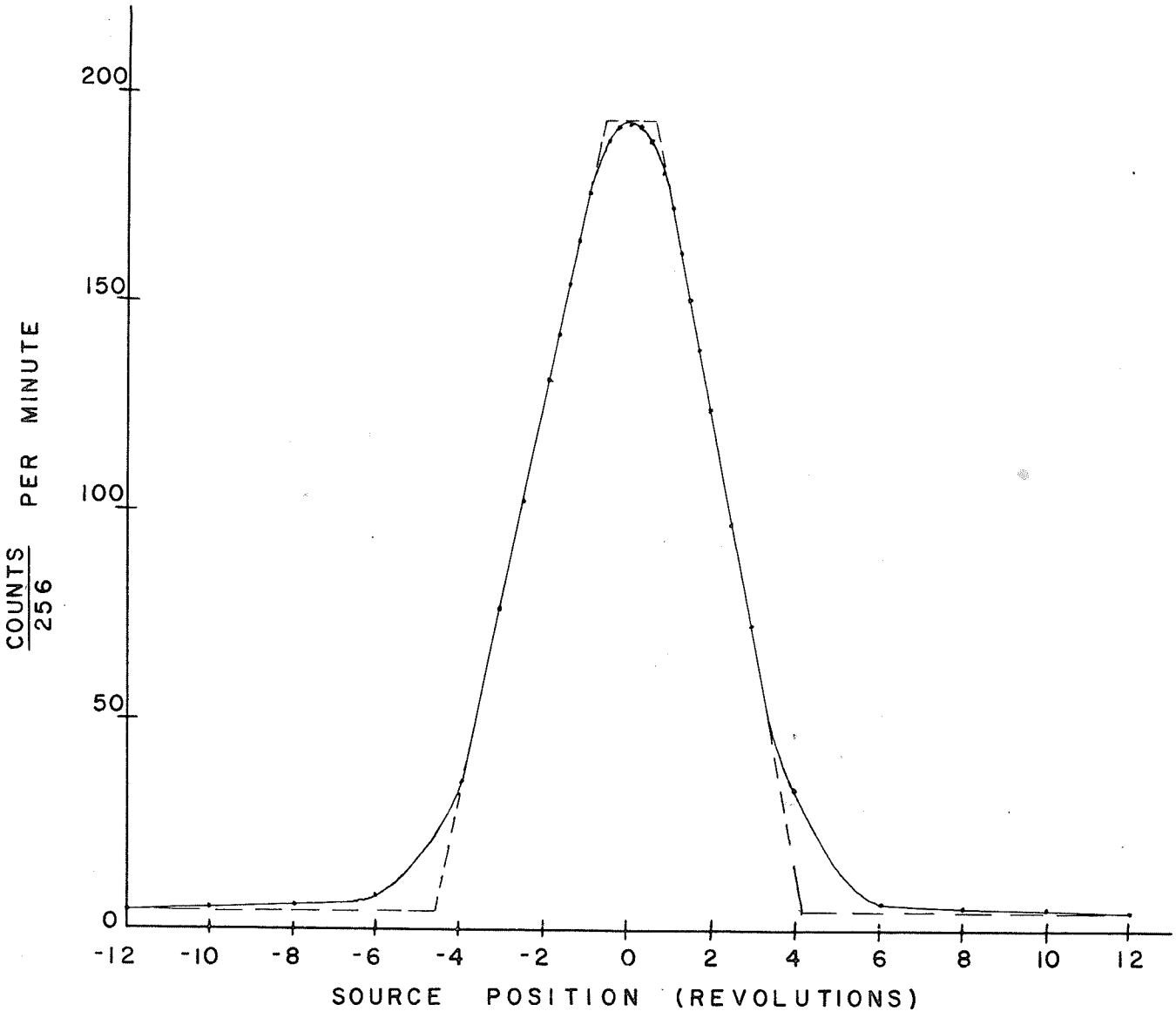

FIG.15 TRANSMISSION CHARACTERISTIC OF THE COLLIMATOR

Thus the spectrometer will be unable to investigate gamma-rays of higher energies than 1.2 Mev, the intense direct beam of radiation masking the selectively reflected spectrum after this point. The low energy limit of the instrument is, of course dictated by the length of the rack in the driving assembly. This corresponds to a low energy limit of approximately 20 kev.

Curved Crystal Alignment

The curved crystal must be mounted on top of the vertical shaft in such a position that its transverse atomic planes, if produced, will intersect in a vertical line at the leading edge of the source. This requires two adjustments. Firstly the crystal must be vertically oriented in its clamping blocks so that the transverse planes [the (310) planes in this case] are vertical, and secondly the curved crystal must be horizontally oriented so that the centre of curvature of the crystal clamping blocks lies on the leading edge of the source.

Since the direction of the (310) planes in the crystal specimen used was known only to within $\pm$ 1°, an exact vertical alignment was impossible. The crystal was therefore mounted in the clamping blocks with its (310) planes approximately vertical, the final adjustment having to wait until the spectrometer was in actual operation.

An optical system was set up to make the horizontal alignment. A hollow cylindrical aluminum capsule was machined to fit snugly into the source aperture. A narrow vertical slit was milled out of this capsule near the bottom, and a

small light bulb inserted so that its filament was opposite the slit. The capsule was now placed in the source aperture so that the slit was in the centre of the entry end of the tapering channel leading out from the source castle, and voltage applied to the bulb. The image of the slit was reflected by the curved crystal and focused on a screen just above the source aperture. The bolt clamping the crystal-mount table to the vertical shaft was loosened, and the table rotated until the image of the slit was focused directly above the slit itself. The table was then locked securely in place, thus keeping the crystal clamping blocks in the correct horizontal alignment.

(II) FINAL ALIGNMENT

The final alignment of the spectrometer was accomplished using a radioactive source of Ir-192 which has a half-life of 74 days. The source, in the form first described in chapter 2, section (II) of this thesis, was produced by pile irradiation at Chalk River, Ontario. The iridium foil which was immersed in the neutron flux of the pile was of a necessarily high purity. It contained only the following impurities: Pt - 0.03%, Pd - 0.003%, Rh - 0.02%, Cu - 0.02%, Fe - 0.02%, Mg - 0.0004%, Mn - 0.0002%, and Si - 0.01%. After a six day irradiation period in the pile the estimated strength of the Ir-192 was of the order of 600 millicuries. This source was mounted in the spectrometer using the technique previously described.

Location of the peaks

The location of the gamma-ray peaks in the spectrum was greatly facilitated by calculating beforehand the approximate spectrometer setting at which they should occur. For example, Dumond[12] quotes 316.46 kev. as the energy of the most intense line in the gamma-ray spectrum of Ir-192. Now for the spectrometer:

$$\sin \theta = \frac{x}{A}$$

where θ = the Bragg angle of reflection

x = the distance, along the rack from the "zero" position, at which the peak occurs.

and A = the length of the constant hypotensue.

Also, for 1st order Bragg reflection:

$$\sin \theta = \frac{\lambda}{2d}$$

where λ = the wavelength of the gamma-ray, and

d = the grating distance of the crystal planes

$$\text{i.e.} \quad \sin \theta = \frac{6.2}{E\ d}$$

where E = the energy of the gamma-ray in kev., if d is in Angstrom units.

Thus, we have $\frac{x}{A} = \frac{6.2}{E\ d}$

$$\text{or } x = \frac{6.2 \times 52.00}{316.48 \times 1.175} \text{ inches}$$

$$= 0.865 \text{ inches}$$

$$\approx 22.8 \text{ revolutions (of the brass driving disc)}$$

Therefore, the most intense peak in the spectrum should occur at a spectrometer setting of 22.8 revolutions if the machine has been correctly aligned, i.e. if the

mechanical "zero" is in fact the "zero" of the wavelength scale.

Before searching for this intense 316 kev peak, the pulse height selector had to calibrated. The source was positioned as close to the "zero" position as possible without saturating the scaler, thus allowing part of the radiation beam to impinge directly upon the scintillating crystal. With the machine set at this position, a scintillation spectrum was taken by varying the bias level of the differential pulse height analyzer. From this spectrum the bias level for the 316 kev. line was determined. It should be noted that this bias level was only approximately correct since the radiation reaching the scintillating crystal was slightly degraded in energy. An exact calibration of the scintillation spectrometer was unnecessary until the curved crystal spectrometer had been fully aligned.

The bias level was now set at 316 kev. and a search made with the curved crystal spectrometer in the region around 22.8 revolutions. The maximum gate of 10.0 volts was used in the scintillation spectrometer to ensure that all of the 316 kev. peak would be counted even if the bias level calibration was slightly in error. The spectrum was explored point by point in the region around 22.8 revolutions, consecutive points being taken close enough together to make sure that the peak did not pass unnoticed. Since Dumond quotes a line width of 0.25 MA^{o} for his machine, which corresponds to approximately one seventh of a revolution of

the driving assembly of the spectrometer under consideration, consecutive readings were taken 0.05 revolutions apart.

When the 316 kev. line was first discovered, as expected, it was extremely wide and completely unresolved from its intense neighbouring lines of energies 308 kev. and 296 kev. To increase the resolution and the peak-to-valley ratio of the spectral lines several parts of the spectrometer had now to be realigned.

Vertical orientation of the curved crystal

The curved crystal must be aligned so that its transverse atomic planes are vertical. The device for orienting these planes has been described in chapter 2, section (III).

Once the 316 kev. line had been located the primary task was therefore to make the (310) planes of the quartz crystal vertical. The direction of these planes was varied a little at a time by rotating the template, which enclosed the crystal, in a vertical plane. To do this the crystal clamping blocks were loosened just enough to allow movement of the crystal. The template was then rotated by turning the calibrated drum, as previously described, and the blocks securely clamped once again. For each setting of the crystal a run was made with the spectrometer over the region of the 316 kev. line.

Great care had to be taken with this alignment to ensure that the crystal did not fracture. It was discovered that, after being tightly clamped in the blocks for a week or more, the quartz crystal tended to adhere to the rubber

gasket making a rotation of the template extremely difficult. Rather than the template and crystal rotating as a single unit, the template tended to ride over the stationary crystal which led to the ultimate fracture of the crystal when the blocks were reclamped. Before the mounting of a new crystal, the rubber gasket was lightly dusted with talcum powder. This was found to be a great improvement although the crystal still tended to adhere to the gasket if tightly clamped for too long a period.

For each spectrometer run a graph of intensity versus wavelength setting was drawn for the 316 kev. line, and the value of the peak width at half-maximum and the peak-to-valley ratio determined. The crystal was then oriented at the drum setting which gave the maximum peak-to-valley ratio and the minimum peak width. At this setting the (310) planes of the crystal were vertically aligned.

As the transverse planes of the curved crystal became closer and closer to the vertical a marked change occured in the nature of the 316 kev. line. The peak-to-valley ratio and the resolution increased rapidly, separating the 316 kev. peak from the neighbouring 308 kev. and 296 kev. lines. In figure (16) graph (a) is a plot of the 316 kev. peak width versus the angle made with the vertical by the (310) planes, and graph (b) is a plot of the peak-to-valley ratio versus the angle made with the vertical. Both curves show the extreme sensitivity of the peak nature to the vertical orientation of the curved crystal. If the alignment of the transverse planes is out by more than $\pm 1^{o}$

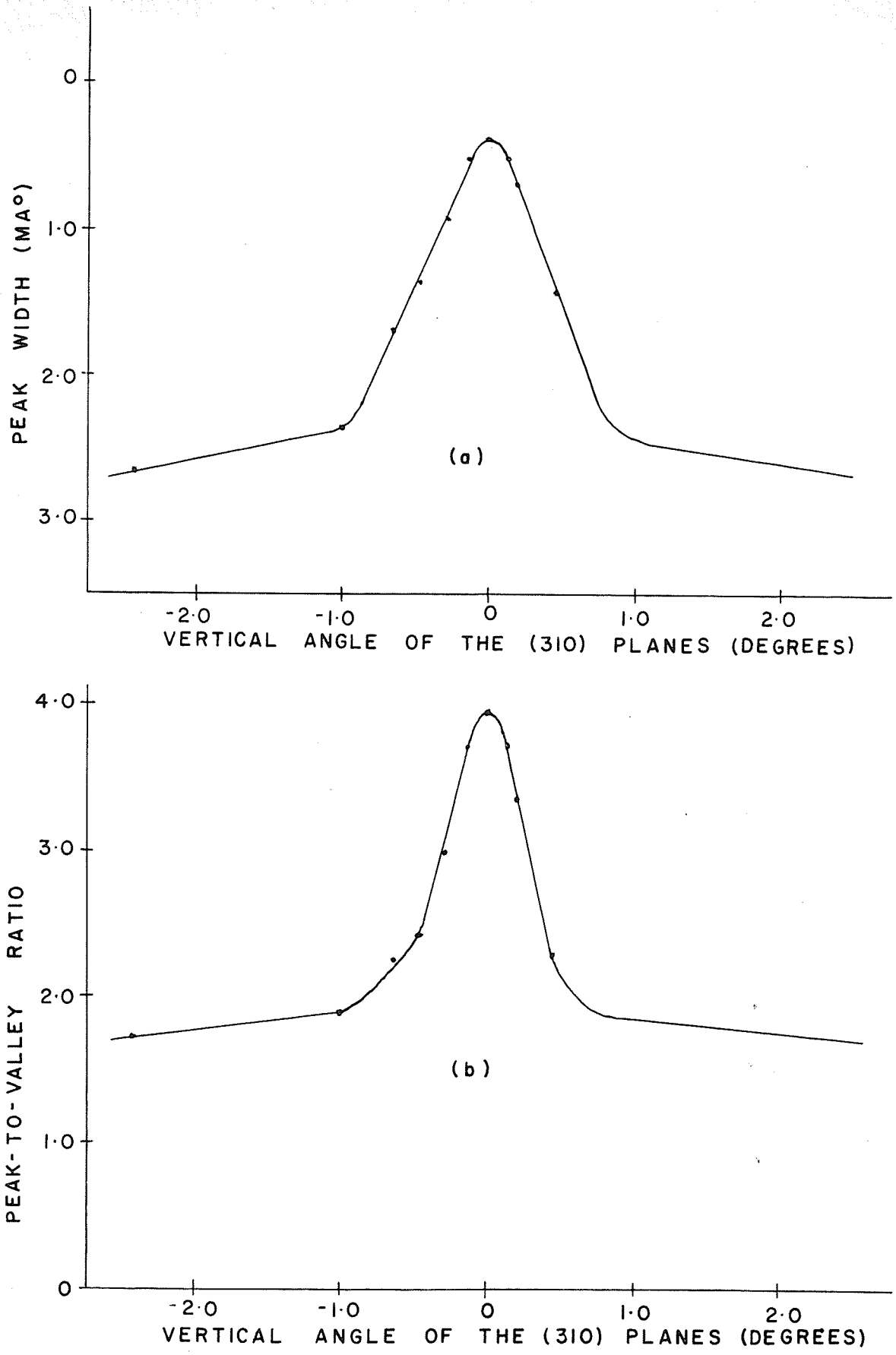

FIG. 16 VERTICAL ORIENTATION OF THE CRYSTAL PLANES

the gamma ray peak is almost undistinguishable from the background. The correct vertical orientation of the curved crystal is therefore of the utmost importance in the overall alignment of the spectrometer.

Orientation of the source

To obtain the best resolution, the source capsule must be oriented in the castle aperture so that the curved crystal views essentially a line source. For this to be the case, the source must be aligned so that the plane intersecting the leading and trailing edges of the iridium foil is perpendicular to the plane of the unstressed quartz crystal. A technique was developed to orient the iridium in this position.

The upper section of the source castle was raised slightly above the lower section by means of thin shims. A long narrow piece of shim stock was now inserted betwwen the two sections. One end of this stock carried a tiny screwdriver blade which fitted snugly into the slot in the head of the source capsule. The other end of the stock protuded outside the castle. By turning the shim stock, therefore, the source capsule, and consequently the iridium foil, could be rotated in the aperture. The amount of rotation was noted on a scale scribed on the outside of the lower castle. For each source position a run was made with the spectrometer over the 316 kev. line.

As in the previous alignment, the peak width at half-maximum and the peak-to-valley ratio of the 316 kev. line was determined for each source capsule position. The

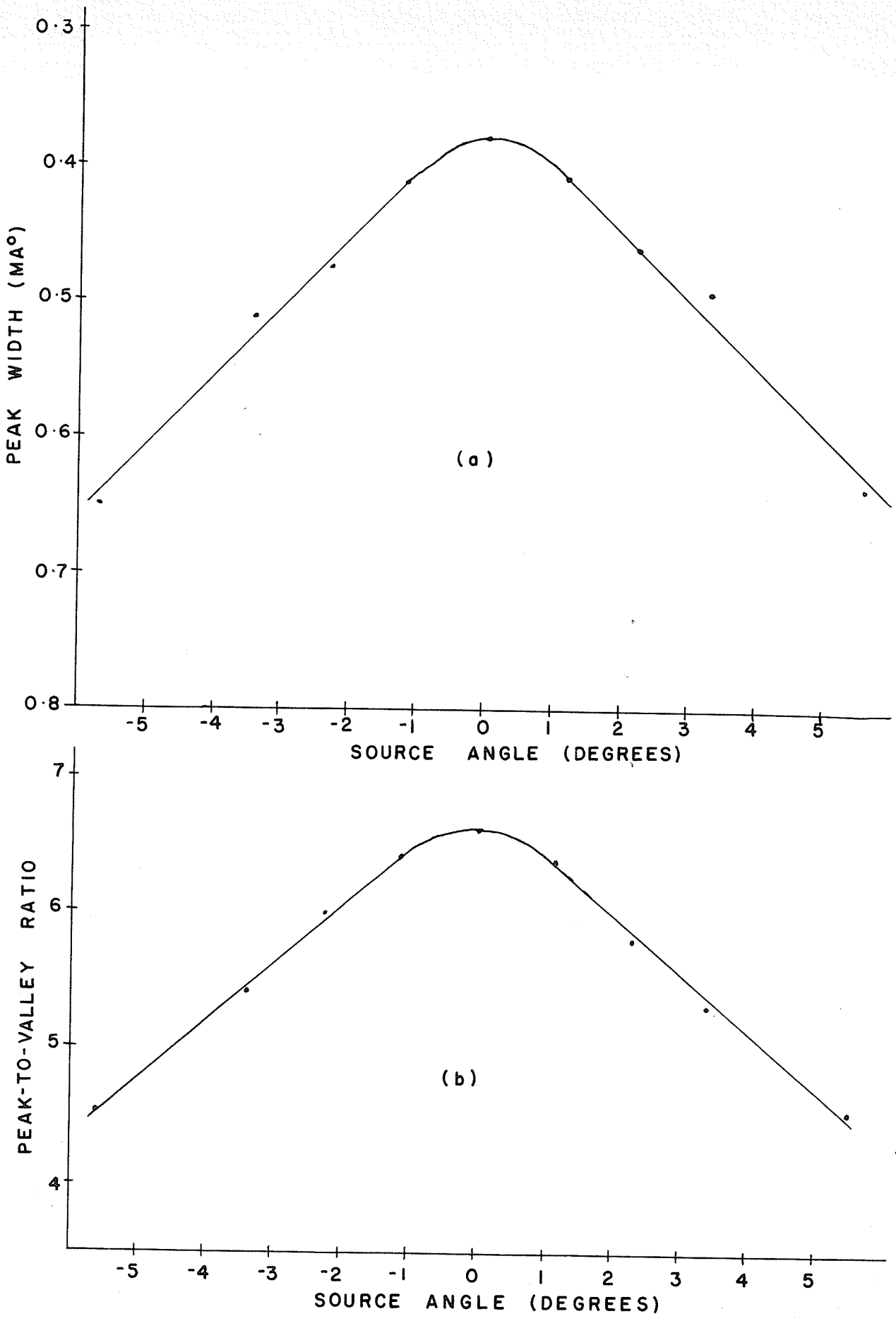

FIG. 17 SOURCE ORIENTATION

source was then placed in the position which gave the maximum peak-to-valley ratio and the minimum peak width. It should be noted that this alignment followed the curved crystal alignment, and consequently one should expect this peak-to-valley ratio to be greater than the maximum peak-to-valley ratio shown in figure (16). Similar considerations follow for the peak-width. In figure (17) graph (a) is a plot of the peak width of the 316 kev. line versus the angular misalignment of the source, while graph (b) is a plot of the peak-to-valley ratio versus the angular misalignment of the source. Comparing these curves with those in figure (16) it can be seen that the nature of the gamma-ray peak is not quite so sensitive to a misalignment of the source as it is to a vertical misalignment of the curved crystal. A misalignment of the source will, however, shift the peak slightly from its estimated position on the wavelength scale. This will, in fact, gradually wipe out the peak all together as the angular misalignment is increased, since the crystal will view an increasing number of very weak line sources side by side rather than a single intense line source.

Alignment of the centre spindle

The centre spindle O which links radius bar I to the lower radial beam II had been approximately aligned as described in the preliminary mechanical alignment. Its position on the lower radial beam had now to be exactly oriented in both longitudinal and transverse directions.

The spindle was firstly unclamped so that it could be moved in only the longitudinal direction along the radial beam. Runs were then made with the spectrometer over the 316 kev. line for various spindle positions, the distances moved by the spindle being noted on a scale clamped to the radial beam. A slight maximum was discovered in the peak-to-valley ratio of the gamma-ray line at a spindle setting of the order of a few millimeters nearer to the curved crystal. The spindle was not clamped at this setting, however, but at exactly half the distance. The radius bar was then shortened by a corresponding amount to ensure that the centre of the spindle was, in fact, the centre of the focusing circle.

Since the centre spindle O is rigidly linked by means of the radius bar II, to spindle C_1 [see figure (5)], a transverse adjustment of this spindle will cause a corresponding rotation of the curved crystal. Spindle O was therefore uncoupled from radius bar II before any adjustment was made in the transverse direction. Runs were made with the spectrometer over the 316 kev. line for various transverse spindle positions. Little or no change, however, could be detected in the nature of the gamma-ray peak for spindle adjustments up to two or three millimeters. Spindle O was therefore reclamped in its original position.

An examination of the 316 kev. line on either side of the mechanical "zero" revealed the lines to be non-symmetrically situated. On the assumption that the pre-set mechanical "zero" is identical with the "zero" of the wave-

length scale and that the curved crystal is accurately focused on the leading edge of the source, this must then be due to the fact that the transverse atomic planes of the crystal are not normal to the crystal slab but intersect the face at a small oblique angle. The centre spindle O must then be pulled to one side until the atomic planes, if produced, intersect at the leading edge of the source. Spindle O was therefore transversely adjusted, while rigidly linked to the spindle C_1, until the 316 kev. lines were symmetrically situated on either side of the "zero" position.

An optical system had to be devised to keep track of the transverse distance moved by the spindle since this distance was less than the order of a millimeter. A parallel beam of light was directed on the curved crystal, and the image of a narrow slit reflected from the crystal to a front-surface plane mirror. The slit image reflected from the mirror was then located in the cross-hairs of a horizontal travelling telescope a few meters to one side of the machine. The distance moved by the spindle was thus noted in terms of the movement of the telescope along its transverse vernier scale. Using this system the 316 kev. lines were symmetrically situated to within 0.2%.

Alignment of the collimator fins

A portion of the background, upon which the gamma-ray lines are imposed, was investigated on either side of the "zero" position using an integral discriminator in the scintillation spectrometer. As is to be expected, each background consisted of a continuous curve increasing in the

high energy direction and rising sharply as the source approached the position at which the direct beam could impinge upon the scintillating crystal. Now, if the lead fins in the collimator are not warped in any way and the collimator is perfectly aligned, the background curves on either side of the "zero" position should be mirror images of each other. It was found, however, that the background curve on one side of the "zero" position was considerably higher than that on the other side for the region examined. The two curves differed from their mean position by as much as 23%. Since the collimator had been previously aligned this could have been caused only by some warp in the baffle structure.

The upper steel plate and lead liner were removed from the collimator, and the fins detected to be slightly bowed at their centres. The brass spacers which hold the fins snugly in the interior of the collimator were removed and filed so that the baffle system could fit loosely into the collimator. The bow in the baffle system was then removed by means of thin shims which became permanent parts of the assembly, and the collimator reassembled.

The background curves were examined once again and showed a considerable improvement. In this case the two curves differed from their mean by only 5%. It is interesting to note that now the two curves had reversed their relative positions, the lower background becoming the higher and vice-versa. It was felt that a 5% difference in background on either side of the "zero" position would not have

too great an effect on the results obtained with the spectrometer, the complete removal of the background difference requiring the time consuming task of rebuilding the entire baffle assembly. The collimator was consequently left in this condition.

Calibration of the scintillation spectrometer

Several runs over the 316 kev. line were made with the curved crystal spectrometer using different gate widths on the differential discriminator of the scintillation spectrometer. The gate width which gave the maximum peak-to-valley ratio was used henceforth in the scintillation spectrometer.

The curved crystal spectrometer was then set at the wavelength corresponding to the 316 kev. line, and a scintillation spectrum taken to determine the e xact bias level corresponding to 316 kev. The bias level corresponding to 468 kev. was similarly determined. From these two values, due to the linearity of the scale, the discriminator level of the pulse height selector could be calibrated in kev. and consequently in revolutions of the brass driving disc on the crystal spectrometer. Thus, in the taking of a complete spectrum on the crystal spectrometer, the discriminator gate could be advanced in conjunction with the brass driving disc.

Chapter 4 - Investigation of the Gamma-Ray and X-Ray Spectra of Ir-192

(I) INTRODUCTION

The n-γ reaction in iridium leads to 74 day Ir-192 and 19 hour Ir-194. The Ir-192 decays by beta emission into Pt-192 and by orbital electron capture into Os-192. The resulting gamma-rays of Pt-192 and Os-192 have been extensively studied[12,15,16,18-23]. The curved crystal spectrometer[12,15,16] has played a major part in the study of these gamma-rays, followed closely by the internal conversion spectrometer (18,19), the external conversion spectrometer[20,21], and the scintillation spectrometer[22,23].

Figure (18) shows the estimated level scheme according to Baggerly et al[12]. It is the result of a careful study of the decay of Ir-192 using a curved crystal spectrometer, an internal conversion spectrometer, and a scintillation spectrometer. The transitions shown as solid lines are those actually detected by Baggerly, while those shown as dotted lines are weak transitions reported by other workers. Of the solid line transitions all were detected in the curved crystal spectrometer except for the 785 kev. and 885 kev. transitions in Pt-192 and the 1060 kev. transition in Os-192. The 885 kev. transition was detected in the beta-ray spectrometer, while the other two transitions were detected only in the scintillation spectrometer.

In table (2) the gamma-ray energies determined by different experimental methods are compared. There appears to be strong agreement in the determined energies except for

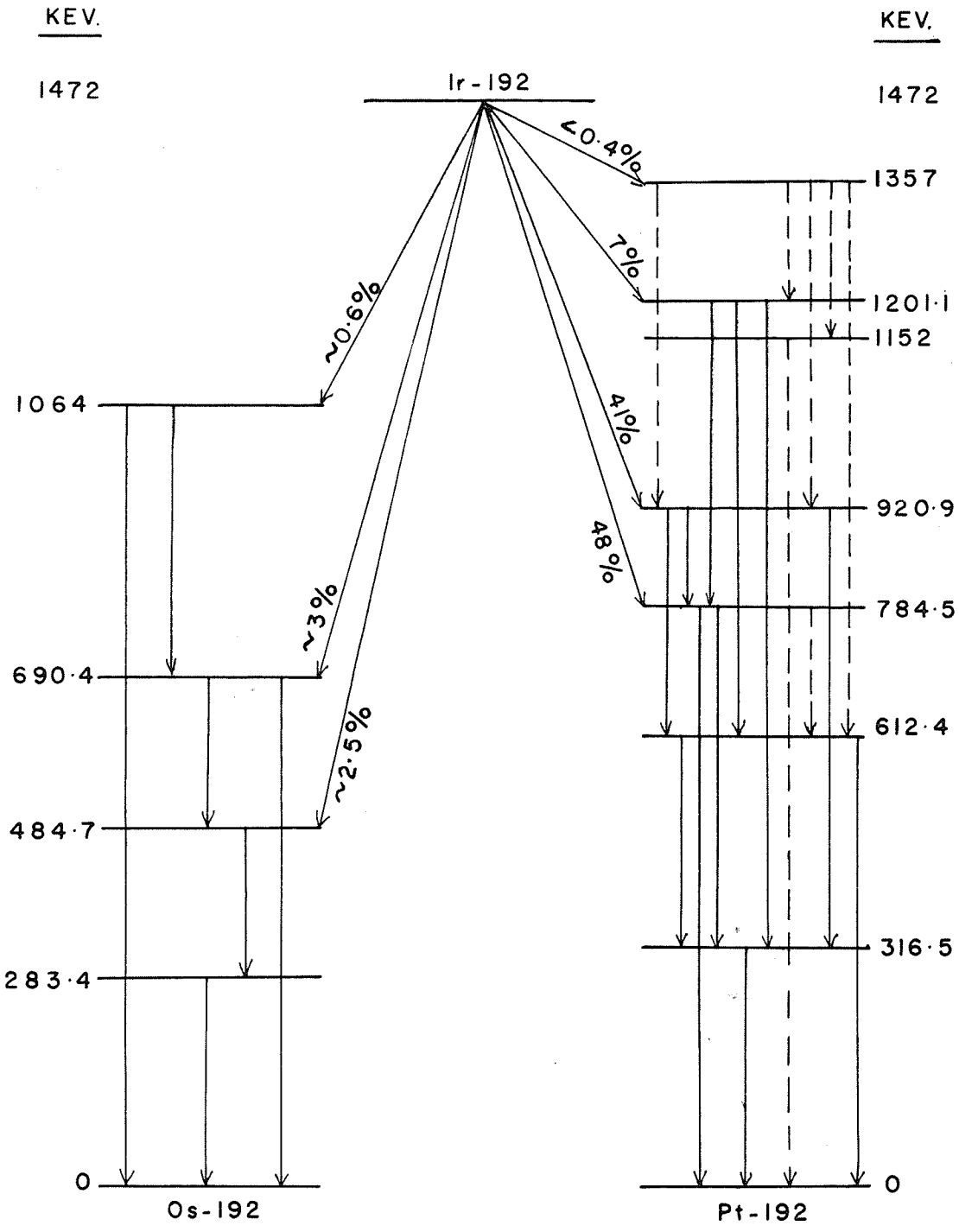

FIG. 18 DECAY SCHEME OF Ir-192 ACCORDING TO BAGGERLY

Table (2): Gamma-ray transitions in PT-192 and in Os-192

Curved Crystal Spectrometer		Internal Conversion Spectrometer		External Conversion Spectrometer
Baggerly[12]	Simbaev[16]	Kalman[18]	Huq[19]	Johns[20]
Energy (Kev)				
-	-	-	45.0(Pt)	-
-	-	-	96.8(Pt)	-
-	-	-	104.7(Pt)	-
136.33(Pt)	-	136.3(Pt)	136.44(Pt)	136.2(Pt)
-	-	-	156.7(Pt)	-
-	-	-	167.5(Pt)	-
-	-	-	-	174.0
201.31(Os)	-	201.3(Os)	-	201.2(Os)
205.75(Os)	206(Os)	205.8(Os)	204.76(Pt)	205.4(Os)
283.35(Os)	-	-	282.5(Pt)	281.5(Os)
295.94(Pt)	296(Pt)	295.9(Pt)	295.3(Pt)	295.8(Pt)
308.45(Pt)	309(Pt)	308.5(Pt)	308.1(Pt)	308.4(Pt)
316.46(Pt)	317(Pt)	316.5(Pt)	315.8(Pt)	316.5(Pt)
374.7(Os)	-	-	-	374(Os)
-	-	-	400.9(Pt)	-
416.6(Pt)	-	-	415.4(Pt)	-
-	-	-	437.35(Pt)	440 ± 2
467.98(Pt)	468(Pt)	468.0(Pt)	466.47(Pt)	467.8(Pt)
484.75(Os)	485(Os)	-	-	484.4(Os)
588.4(Pt)	588(Pt)	-	-	588.7(Pt)
604.5(Pt)	605(Pt)	604.5(Pt)	-	604.5(Pt)
612.9(Pt)	613(Pt)	-	-	612.7(Pt)
-	-	-	-	745 ± 3
785 ± 20	-	-	-	783(Pt)

Table (2): continued

Curved crystal Spectrometer		Internal Conversion Spectrometer		External Conversion Spectrometer
Baggerly[12]	Simbaev[16]	Kalman[18]	Huq[19]	Johns[20]
Energy (Kev)				
885(Pt)	-	-	-	885.4(Pt)
1060±30	-	-	-	1065±2 (Os)
-	-	-	-	1157±2(Pt)

Huq's values. At high energies these are inclined to be lower than the average values. It is the author's opinion, however, that the difference between Huq's values and the average values is due to a calibration error in his machine, since his value of 136.44 kev., which is close to the energy of his calibration line, agrees well with the results of the other researchers. It is interesting to note that Huq lists several low energy gamma-rays which have not been detected by Baggerly, Johns, etc. A possible explanation of this is the fact that Huq used as his source of radiation Pt-192 due to a p-6n reaction in Au-197. The Hg-192, which is the direct result of this reaction decays by positron emission and orbital electron capture to Au-192, which in turn decays to Pt-192 by orbital electron capture. Thus, levels which are excited in Pt-192 formed by this reaction may not be excited in Pt-192 produced by beta emission in Ir-192. It was considered worthwhile, however, to investigate the existence of these low energy gamma-rays in Ir-192, and the results of this will be discussed in a later section.

Although the energies of the gamma-rays resulting from the decay of Ir-192 are well established, there appears to be some disagreement over their relative intensities. Table (3) shows the values of the most reliable relative intensities quoted by researchers in this field. The values for the relative photon intensities of the strong gamma-ray transitions agree at least to within 20%. The values for the relative photon intensities of the weak gamma-ray transitions, however, differ quite substantially, in many cases

by as much as a factor of two. The most outstanding conflict occurs between the values quoted by Johns[16] and by Baggerly[12] for the intensity of the 136.6 kev. photon relative to the 316.5 kev. photon. Johns quotes this value as 34, while Baggerly quotes it as 1.8, a factor of 19 smaller. Obviously there is scope for much work in this aspect of the decay of Ir-192.

The wavelengths of the X-rays which follow the decay of Ir-192 are known to a high degree of accuracy from the theoretically calculated electron binding energies, and have been experimentally verified by Dumond[13]. Dumond quotes the intensities of the K-spectra of osmium, iridium, and platinum as having the ratio 1:1.7:1.3. The iridium X-rays are excited by fluorescent absorption of gamma-rays in the source, while those of platinum and osmium are produced by internal conversion of the gamma-rays following beta-emission and orbital electron capture respectively.

The 19 hour Ir-192 resulting from the n-γ reaction in iridium decays by beta emission into Pt-194. Due to the short half-life of this decay, the resulting gamma-rays in Pt-194 have not been studied to any great extent. An intense gamma-ray transition has been detected both in a curved crystal spectrometer[15] and in an external conversion spectrometer[20]. The energy of this transition has been quoted as 329.1 kev. and 328.1 kev. respectively.

Table (3): Relative photon intensities of the gamma-ray transitions following the decay of Ir-192

Energy (Kev.)	Relative Intensities			
	Baggerly[12]	Simbaev[16]	Johns[20]	Bashilov[21]
136.3	1.8	-	34	-
201.3	4.6	-	11	-
205.6	39	49	45	35
283.4	5.8	-	13	-
295.9	360	371	340	390
308.5	350	379	360	403
316.5	1000	1000	1000	1000
374.7	18.4	-	6.5	-
416.6	16.2	-	-	-
468.0	640	610	740	533
484.8	39	56	63	-
588.4	70	66	83	43
604.5	140	118	130	130
612.9	84	92	100	53

N.B. The above sets of readings were normalized using the intense 316.5 kev. line

(II) PROCEDURE

The gamma-ray spectrum of Ir-192 was obtained using the strong source described in the previous chapter. This spectrum was explored point by point on either side of the "zero" position of the spectrometer. As a double check against backlash the radial beams were driven in only one direction along the tracks from the beginning to the end of the spectrum. As the spectrum was scanned by the curved crystal spectrometer, the differential bias level in the scintillation spectrometer was varied so that the pulse height selector gate admitted only pulses having the same energy as the gamma-rays reflected according to the Bragg relation by the curved crystal. In this manner, a large fraction of the spurious pulses due to cosmic rays and scattered gamma-rays were removed from the spectrum. For each setting of the curved crystal spectrometer the intensity of the reflected beam was measured by determining the number of counts registered by the scaler over a period of time varying from five minutes to one hour. The counting periods were long in the region of the gamma-ray peaks and in regions of the spectrum where the counting rate was low. The counting periods were short in the background regions of the spectrum and in regions where the high counting rate gave sufficiently good statistics. Graphs of intensity versus wavelength were drawn up for the spectra on either side of the "zero" position and will be discussed in the following section. All of the gamma-rays detected by Baggerly in his 2-meter spectrometer were detected in the

spectrometer under consideration.

It was discovered that this first source of Ir-192 was very inefficient at the low energy end of the spectrum. At low energies self-absorption in the source made it extremely difficult to locate the gamma-ray peaks which were considerably reduced in intensity. To overcome this problem a second source was designed as described in chapter (2), section (11). In this case the iridium was irradiated for 29 days in the neutron flux of the pile at Brookhaven National Laboratories, New York. Since the source was mounted in the spectrometer approximately 21 hours after removal from the pile an attempt was made to locate the 328 kev. transition in Pt-194. This attempt proved successful.

Using this second source the X-ray spectrum of Ir-192 was carefully examined in a manner similar to that used in the investigation of the gamma-ray spectrum. This time, however, the "zero" of the wavelength scale was determined only by the positions of the intense 316.5 kev. gamma-ray transition, and the X-ray spectrum taken on only one side of the mechanical "zero". An examination of the results obtained with the first source will show this to be quite acceptable. The X-rays detected by Dumond[13] were verified, and a $K\beta_3$ X-ray in iridium which was unlisted by Dumond, also found.

Due to the strength of the second source the four most intense peaks in the Ir-192 gamma-ray spectrum were obtainable in second order, and were to prove very useful in the ultimate calibration of the spectrometer.

(III) RESULTS

Gamma-ray spectrum of Ir-192

The gamma-ray spectrum produced using a scintillation spectrometer in tandem with the curved crystal spectrometer was of a very curious nature. The gamma-ray lines themselves were narrow, sharply-rising peaks which is to be expected. Using a differential pulse height analyzer in the scintillation spectrometer, however, it is to be expected that these lines lie on a low, almost constant background curve, this was not the case.

Figure (19) is a view of the complete gamma-ray spectrum of Ir-192 observed on one side of the "zero" position. The spectrum produced by reflection from the other side of the crystal planes is simply a mirror image of this plot except that the centre of symmetry of the two halves is slightly to one side of the mechanical "zero" position as has been previously discussed. Since the scale of this plot is highly compressed, the gamma-ray peaks are depicted by narrow vertical lines, the heights of which approximately represent the line intensities.

Consider the background upon which these lines are imposed. The intense 468 kev. line and the intense 300 kev. triad sit on top of two background "humps". The portions of these "humps" on the low energy side of the peaks could perhaps be explained by degraded compton radiation from the intense gamma-ray lines, but no satisfactory explanation was immediately readily apparent for the portions of the "humps" on the high energy side of the peaks. In the belief that

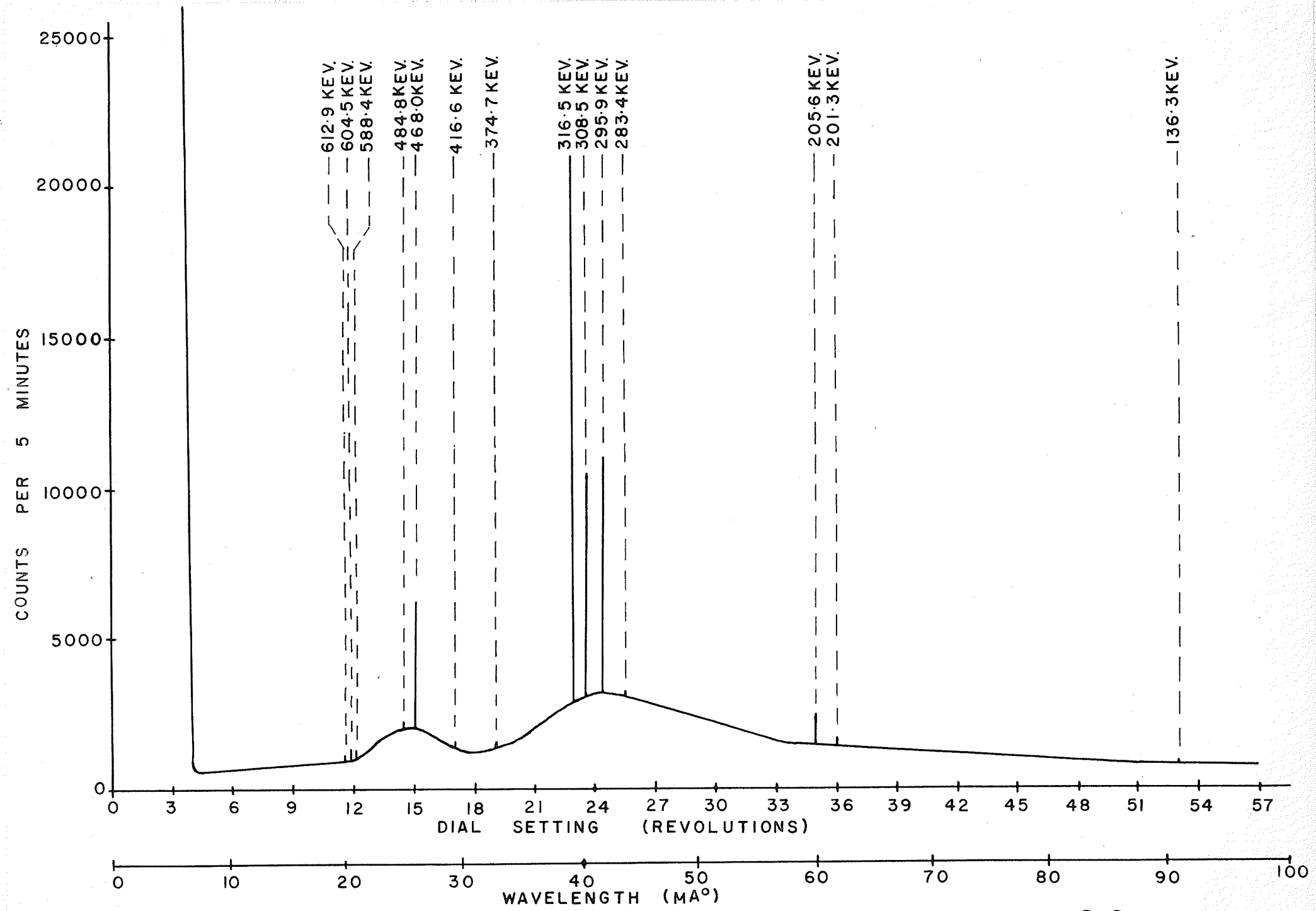

FIG. 19 GAMMA-RAY SPECTRUM OF Ir-192

this effect was largely instrumental a check was made to ensure that it was not caused by a change in the curvature of the crystal across the aperture of the clamping blocks. Approximately one centimeter was masked with lead from each side of the aperture and the results so obtained compared with those obtained using the entire aperture. Little or no change could be noticed in the background curve, although a radical change occured in the peak nature. The peak width, for example, was reduced by the order of 10%, and the peak-to-valley ratio reduced by the order of 15%. The probable explanation for this background curve will be discussed in the final section.

For the actual gamma-ray lines observed with the spectrometer the peak width at half-maximum was 0.28 MA^{o}, or approximately 25 seconds of arc. The variation of peak width with energy was too small to detect. Figure (20) is a plot of intensity versus dial setting for the intense 300 kev. triad in platinum. It shows the excellent resolution obtained with the spectrometer in this energy region.

X-ray spectrum of Ir-192

The X-ray spectrum obtained with the spectrometer was of a slightly different form than the gamma-ray spectra. The peak nature, for example, was quite different. The X-ray peaks were much broader than the gamma-ray peaks, having a peak width at half-maximum of 0.50 MA^{o} as compared with 0.28 MA^{o} for the gamma-ray peaks. Also, the background curve upon which the X-ray lines are superimposed is essentially constant. In figure (21) a comparison is made between a typical X-ray peak and a typical gamma-ray peak.

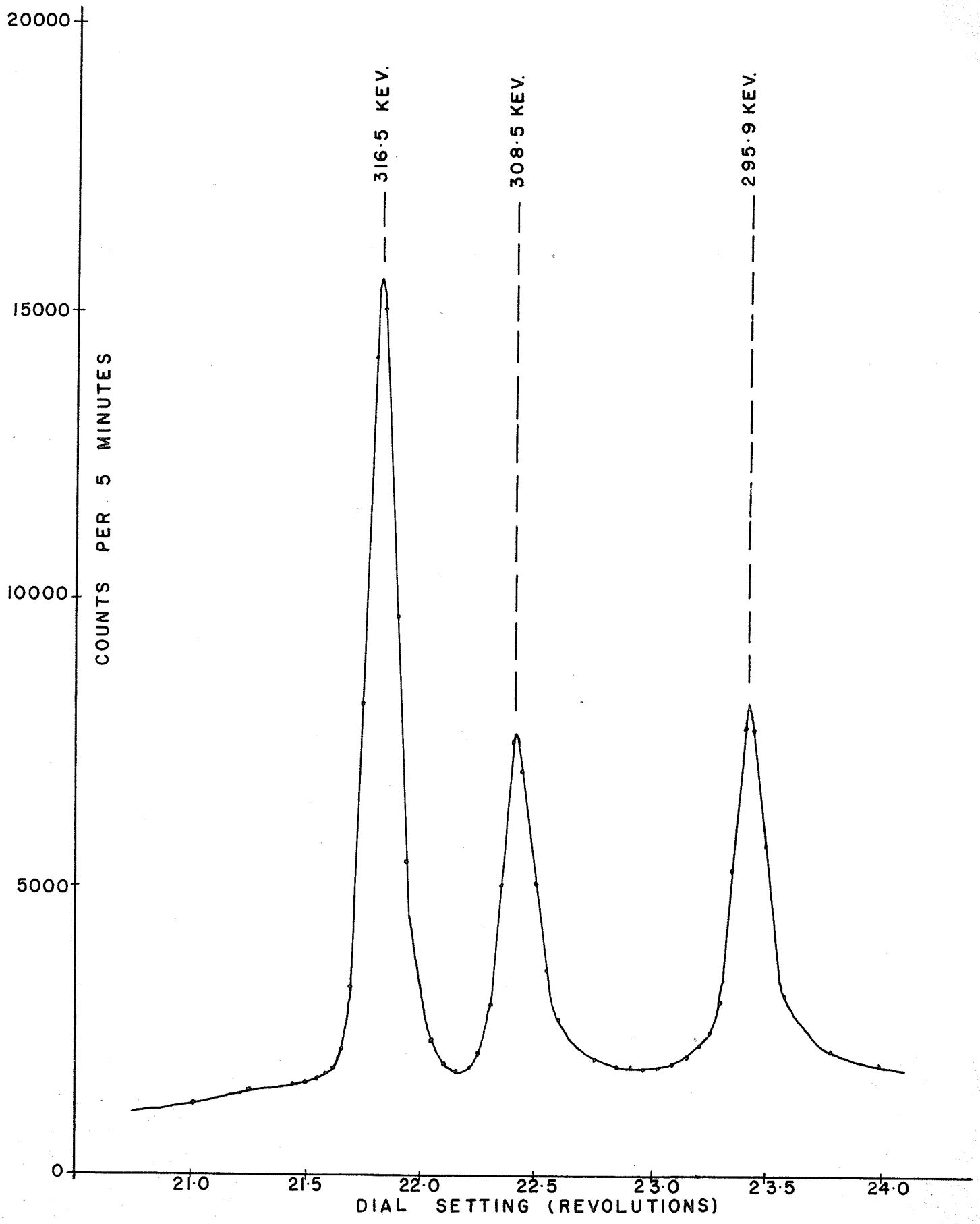

FIG. 20 INTENSE PLATINUM TRIAD

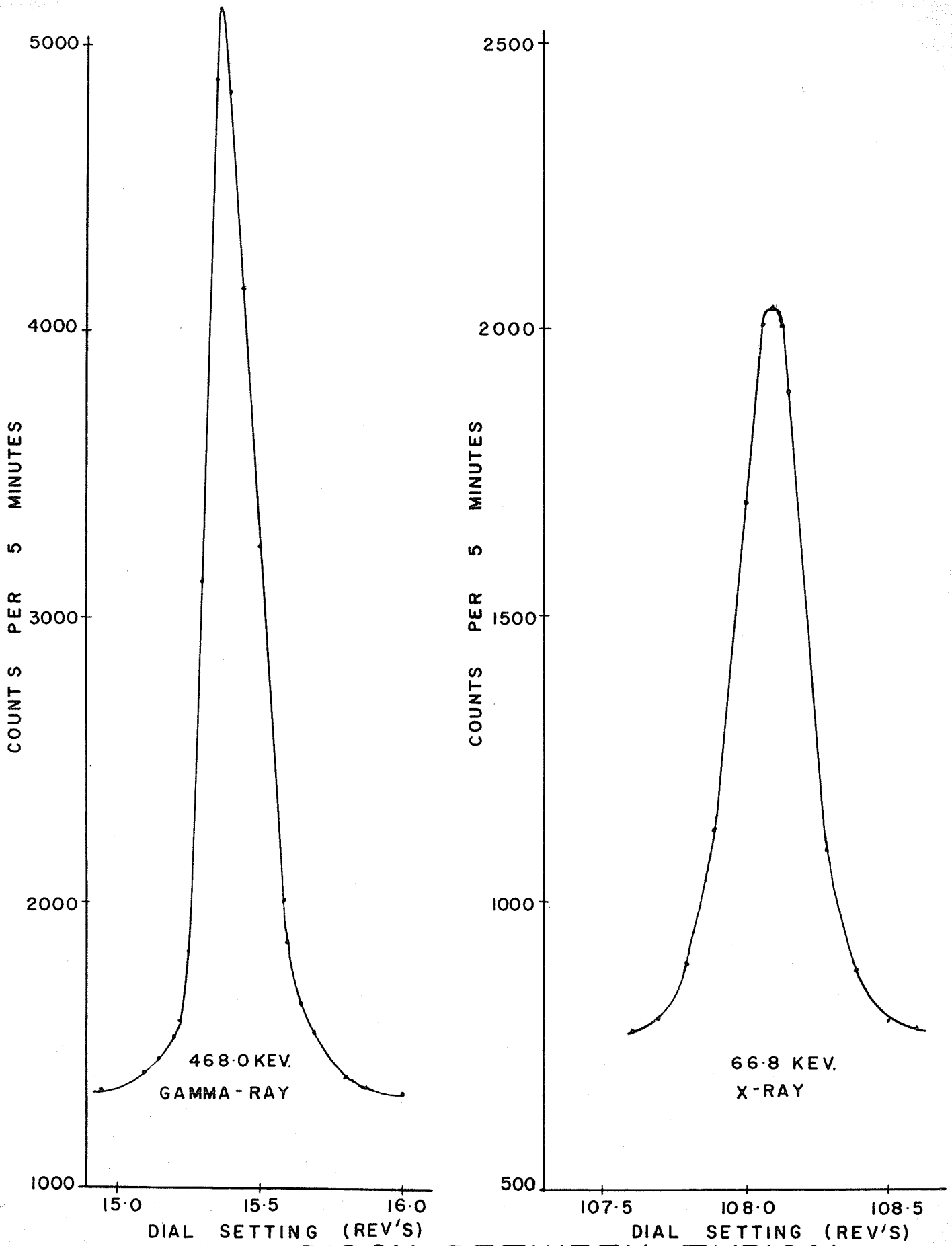

FIG. 21 COMPARISON BETWEEN TYPICAL GAMMA AND X-RAY PEAKS

Wavelength Calibration of the Spectrometer

The primary use of the gamma-ray and X-ray spectra of Ir-192 was to calibrate the curved crystal spectrometer. If the machine has been accurately aligned and the rack and pinion system has linear characteristics, then the wavelength of the spectral lines should be directly proportional to the dial setting of the brass driving disc.

$$\text{i.e. } \lambda = KD$$

Using the known values of λ and the experimentally determined values of D, the proportionality constant K was therefore calculated for each value of λ and D.

Table (4) is a list of the calculated values of K. The dial settings D_A and D_B are the positions of the peak maxima on either side of the mechanical "zero" of the spectrometer. The dial settings D are the distances of the peak maxima from the true "zero" of the wavelength scale. The wavelength values are those due to Baggerly et al[12]. The errors listed for the values of K were calculated using both the estimated error in the determined values of D and the errors quoted by Baggerly in the values of λ. Baggerly quotes one twentieth of the peak width and one fifth of the peak width as the possible errors in the wavelengths of the intense lines and weak lines respectively. Since the width of the peaks detected in Baggerly's spectrometer and the width of the peaks detected in the spectrometer under consideration are quite comparable, the same error was assigned to the estimation of the peak position.

Figure (22) is a graph of the proportionality constant versus the dial setting. In this plot the error in

Table (4): Calculated values of the proportionality constant linking dial setting with wavelength

Dial Setting (revolutions) D_A	D_B	D	Wavelength (MA°)	Nature of the spectral line	K (MA°/rev)
11.59	11.79	11.69	20.224	1st order	1.7300 ± .0051
11.76	11.96	11.86	20.506	1st order	1.7290 ± .0052
12.10	12.28	12.19	21.068	1st order	1.7293 ± .0035
14.72	14.68	14.79	25.573	1st order	1.7291 ± .0016
15.27	15.39	15.33	26.489	1st order	7.7279 ± .0016
17.20	17.30	17.25	29.753	1st order	1.7248 ± .0058
19.16	19.28	19.22	33.080	1st order	1.7211 ± .0045
22.00	-	21.93	37.721	1st order *	1.7201 ± .0020
22.73	22.83	22.78	39.172	1st order	1.7196 ± .0010
23.32	23.42	23.37	40.189	1st order	1.7197 ± .0010
24.32	24.42	24.37	41.888	1st order	1.7188 ± .0010
25.35	25.45	25.40	43.744	1st order	1.7178 ± .0024
30.91	-	30.84	52.978	2nd order	1.7178 ± .0024 *
35.04	35.14	35.09	60.254	1st order	1.7171 ± .0006
35.93	-	35.86	61.587	1st order	1.7174 ± .0006
45.70	-	45.63	78.344	2nd order	1.7169 ± .0015

* This is the intense gamma-ray transition in Ir-194

Table (4): - continued

Dial Setting (revolutions) D_A	D_B	D	Wavelength (MA°)	Nature of the spectral line	K (MA°/rev)
46.87	-	46.80	80.378	2nd order	1.7174 ± .0015
48.85	-	48.78	83.776	2nd order	1.7172 ± .0016
52.90	53.00	52.95	90.929	1st order	1.7172 ± .0005
92.81	-	92.74	159.257	$K\beta_2$(1),(11)Pt	1.7172 ± .0002
95.42	-	95.35	163.661	$K\beta_1$ Pt	1.7164 ± .0002
95.84	-	95.77	164.463	$K\beta_3$Pt	1.7173 ± .0002
98.21	-	98.14	168.524	$K\beta_1$Ir	1.7172 ± .0002
98.66	-	98.59	169.307	$K\beta_3$Ir	1.7173 ± .0002
101.15	-	101.08	173.584	$K\beta_1$Os	1.7173 ± .0002
101.61	-	101.54	174.418	$K\beta_3$Os	1.7173 ± .0002
108.09	-	108.02	185.485	$K\alpha_1$Pt	1.7171 ± .0002
110.90	-	110.83	190.362	$K\alpha_2$Pt	1.7176 ± .0002
111.30	-	111.23	191.031	$K\alpha_1$Ir	1.7174 ± .0002
114.13	-	114.06	195.869	$K\alpha_2$Ir	1.7172 ± .0002
114.67	-	114.60	196.771	$K\alpha_1$Os	1.7171 ± .0002
117.48	-	117.41	201.620	$K\alpha_2$Os	1.7172 ± .0002

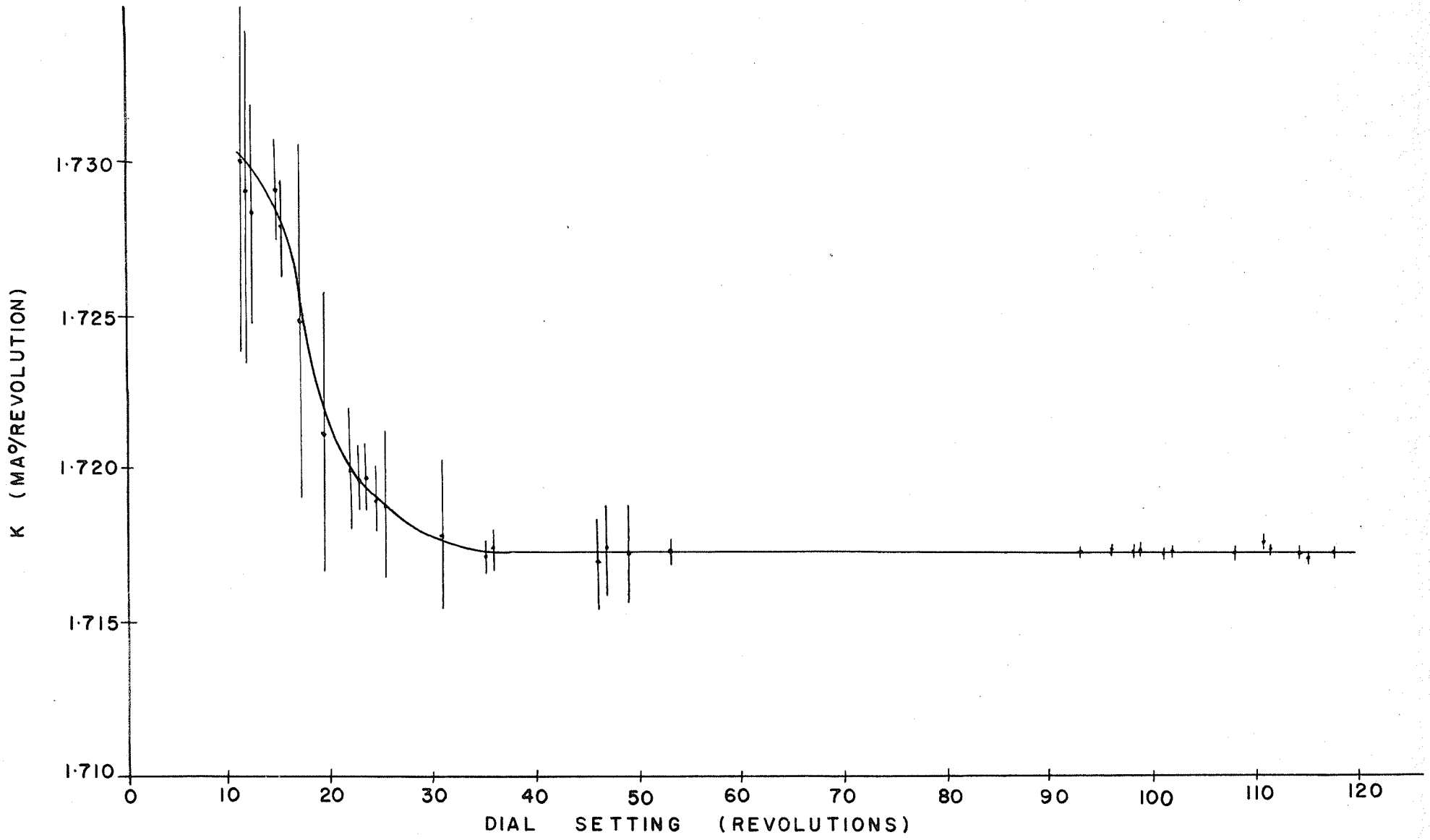

FIG. 22 WAVELENGTH CALIBRATION CURVE

K is shown by a vertical line through each point. The error in the dial setting is negligible on this compressed scale. If the machine is accurately aligned and the rack is uniform, then the curve should be a horizontal line. This appears to be the case below 200 kev. Above this energy, however, the curve rises slightly, the maximum rise being approximately 0.75%. A tentative explanation of this will be discussed in the final section. Certainly, however, the rack and pinion system appears to behave in a very uniform manner as shown by the very small scatter of the points. For the spectral region below 200 kev., therefore, it is conservatively estimated that the value of K can be determined to within one part in five thousand. For the spectral region above 200 kev. it is estimated that the value of K can be determined to within one part in eight hundred. This decreases in the precision of determing K is due partly to the rising of the curve and partly to the increase in the errors assigned to the points on the curve. The estimate is based largely upon the allowable scatter in the points determined by the more intense gamma-ray transitions such as the 468 kev. line and the 300 kev. triad.

Relative Photon intensities

In calculating the spectral sensitivity of the curved crystal spectrometer the following effects must be considered: the efficiency of the scintillation spectrometer used as a detector of the gamma-radiation, the reflection efficiency of the curved crystal, and self-absorption in the source.

In table (5) the relative photon intensities of the gamma-ray transitions are shown at each stage of their correction. I_1' and I_1'' are the raw relative intensities observed on either side of the "zero" position. These were obtained by subtracting the background from the gamma-ray lines and taking the counting-rates at the tops of the peaks. This is justified by the fact that the peak shape does not vary appreciably throughout the spectrum. I_1 is the mean of I_1' and I_2'' normalized so that the 316 kev. has a relative photon intensity of 1000.

The values labelled I_2 are the relative photon intensities corrected for the reflection efficiency of the curved crystal. The reflection coefficient for the (310) planes in quartz is given by Simbaev[16] as

$$\Gamma_i = k\, E^{-n}$$

where k = constant of proportionality

E = the energy of the gamma-ray transition

and $n = 1.85 \pm .04$.

Thus $I_2 = E^{1.85}\, I_1$.

The values of I_1 were consequently corrected for the variation of the reflection coefficient with energy.

The values labelled I_3 are the relative photon intensities corrected for the efficiency of the scintillation spectrometer. The total detection efficiency of a scintillation spectrometer is a product of two factors: the efficiency of the scintillating crystal and the photopeak efficiency, each of which is a complicated function of energy. These functions have been computed for various crystal sizes.

The information used to obtain I_3 was taken from a compilation of such results by Mott and Sutton[24].

Unfortunately, a quantitative treatment of self-absorption proved beyond the scope of this thesis, due to the geometry of the first source. An attempt was therefore made to obtain sufficient information to make a definite statement concerning the relative photon intensities which show poor agreement to date. In table (5) the column labelled Ia contains the average values of those relative intensities in table (3) which agree to within at least 20%. It should be noted that the values of Ia are obtained from intensity values computed by completely different methods and as such should be more accurate than the results computed by any one method. The ratios of Ia to I_1 were consequently plotted against energy in an attempt to obtain an intensity calibration curve. This curve is shown in figure (23). The values for the relative photon intensities which show poor agreement were thus determined from this graph, and are listed in table (5) under the column labelled I. The validity of these results will be discussed in the final section.

Of the low energy gamma-ray transitions reported by Huq and by Johns [see table (2)] time permitted a careful investigation of only those four shown in table (6). These transitions, if present, were indistinguishable from the background, thus allowing upper limits to be placed on their relative photon intensities. These upper limits are listed in table (6) using symbols identical with those in table (5). The limits denoted by I_1' correspond to twice

the statistical fluctuation of the counting rate in the neighbourhood of the peaks. The estimation of the upper limit on the relative photon intensities of the transitions is probably a little high. It was felt, however, that no definite statement could be made concerning a peak which was lower in intensity then this. Certainly had the peaks exceeded twice the statistical fluctuation of the background counting rate they would have been easily detectable.

Table (5): Relative photon intensities of the gamma-ray transitions

Photon energy (Kev)	Relative Photon Energies I_1'	I_1''	I_1	I_2	I_3	I_a	I
136.3	0.43	0.30	2.0	0.4	0.3	-	1.8
201.3	1.72	1.02	7.5	3.2	2.7	-	6.8
205.6	10.63	6.38	46.6	21.1	18.3	42	-
283.4	1.20	0.94	6.0	4.9	4.6	-	5.2
295.9	85.0	63.0	412	365	353	365	-
308.5	82.0	61.0	399	380	378	373	-
316.5	210.0	149.8	1000	1000	1000	1000	-
374.7	1.39	0.98	6.6	9.0	9.5	-	8.9
416.6	0.80	0.77	5.0	8.4	9.0	-	8.9
468.0	47.3	41.0	249	482	540	631	-
484.8	2.1	1.89	11.3	24.9	28.2	-	34.5
588.4	2.08	1.68	10.6	33.4	40.6	65	-
604.5	4.05	3.37	20.9	69.3	84.9	130	-
612.9	2.41	2.03	12.5	42.5	48.8	82	-

Table (6): Upper limits on the relative photon intensities of some weak gamma-ray transitions reported by Huq and by Johns

Photon energy (Kev)	Relative photon intensities I_1'	I_1	I
156.7	0.2	0.95	0.8
167,5	0.2	0.95	0.8
174	0.2	0.95	0.8
400.9	0.2	0.95	1.4

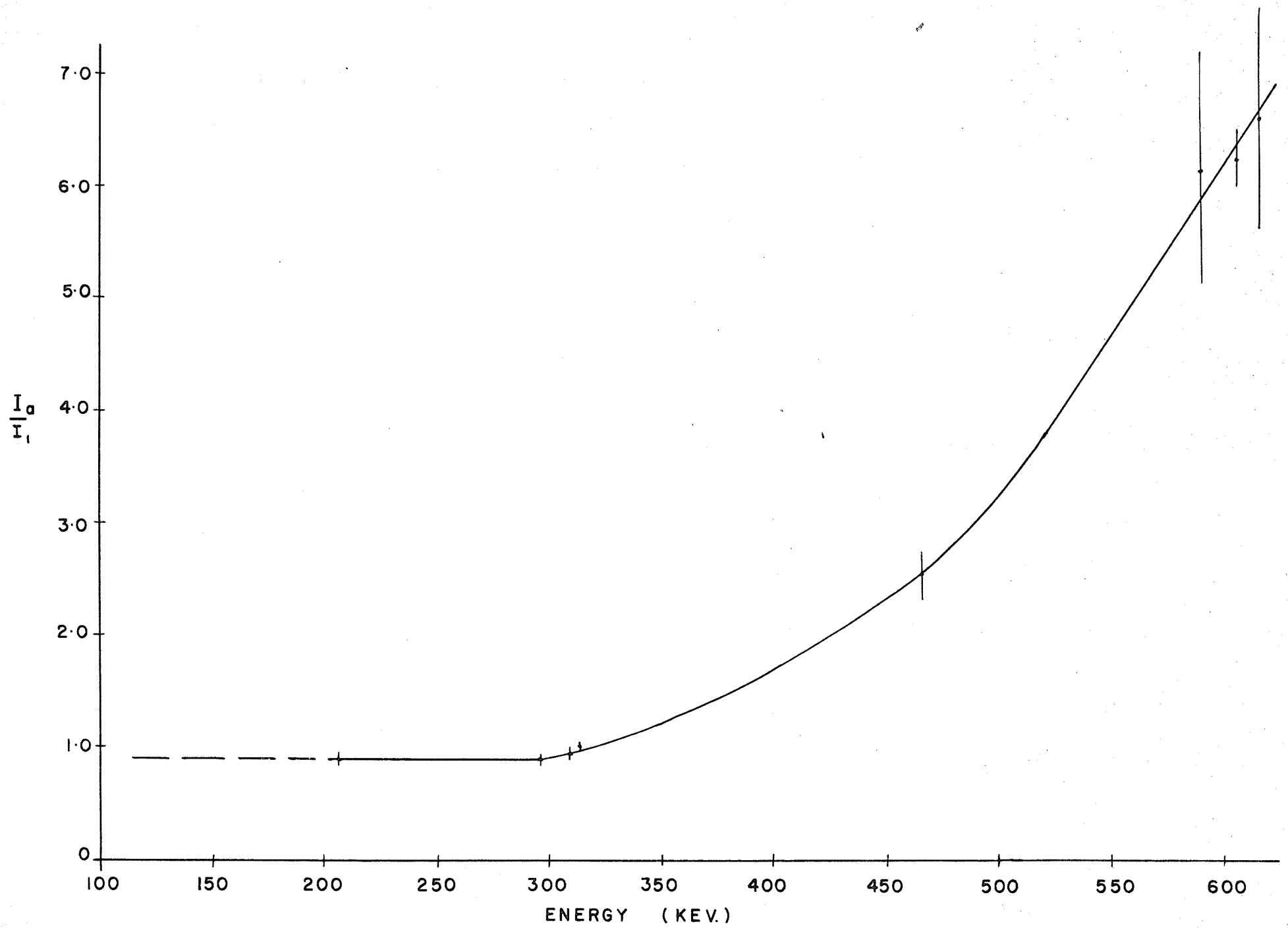

FIG. 23 INTENSITY CALIBRATION CURVE

Chapter 5 - Discussion of Results

(I) PERFORMANCE OF THE SPECTROMETER

On the whole, the performance of the spectrometer was satisfactory. There are several features of the instrument, however, which must be reconsidered in the light of the results obtained.

The primary concern was the calibration of the driving assembly against wavelength. As previously described, the distance moved along the rack is directly proportional to wavelength only in the spectral region below 200 kev. Above 200 kev. the proportionality constant linking dial setting with wavelength increases. A tentative explanation has been formulated for this behaviour of the instrument. Consider figure (24) which shows the geometry of the spectrometer.

let $B'B = BR' = D$

$CB' = L$, $CR' = L'$

and $\angle B'BC = \alpha$

If the machine has been correctly aligned, then

$$\alpha = \pi/2$$

$$L = L'$$

and $$\theta = \theta'$$

Suppose that the original alignment was such that the radial beam CB did not enter the carriage at right angles, i.e. $\alpha = \pi/2 - \varepsilon$ where ε is some small angle. If this were the case, then the spectrometer would experience a slight strain when the source was driven out from the mechanical "zero" position. This would cause either $BB' \neq BR'$ or $L \neq L'$.

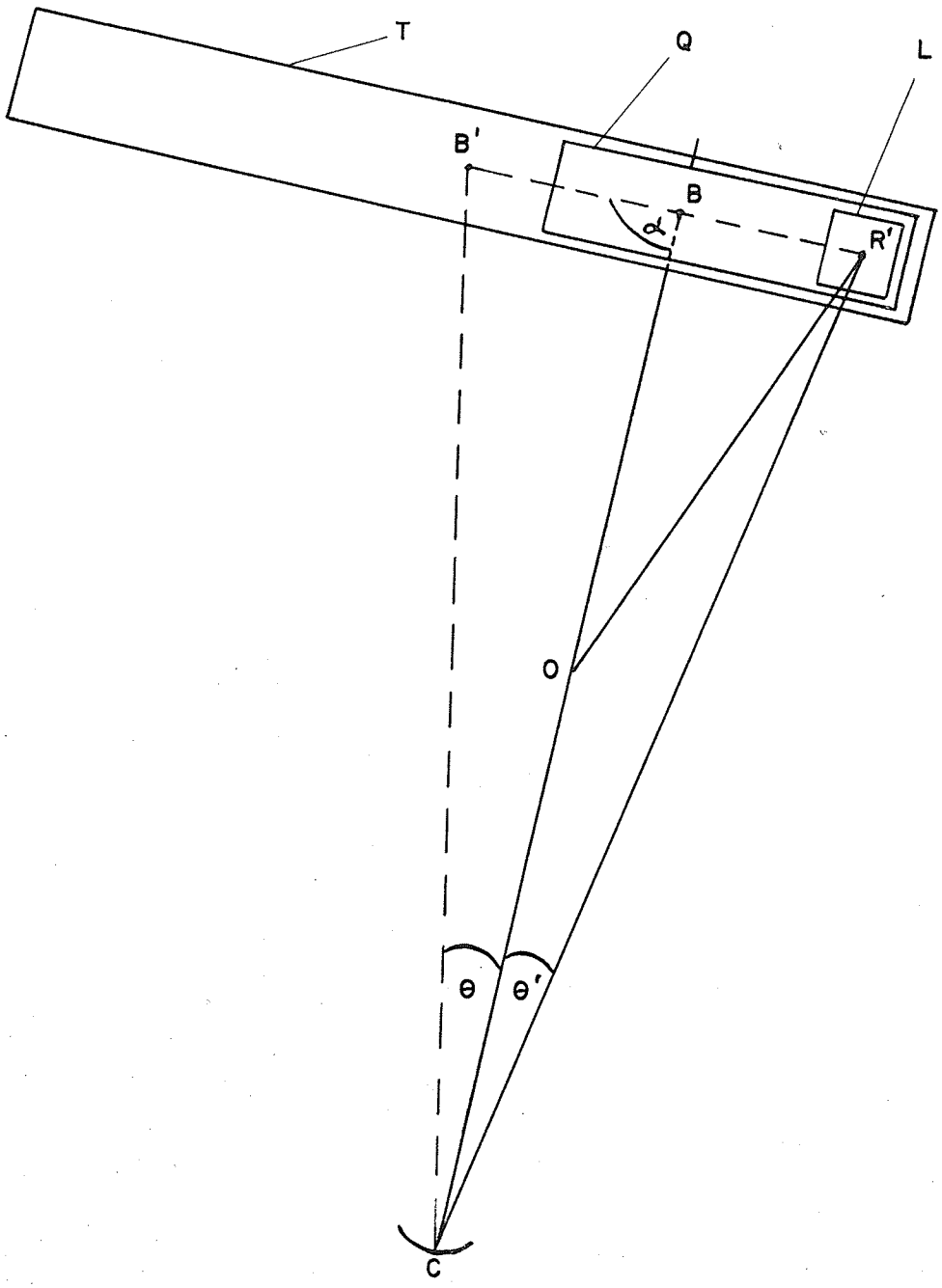

FIG. 24 GEOMETRY OF THE SPECTROMETER SHOWING POSSIBLE MISALIGNMENT

Thus, we have L fixed and L' varying as θ varies.

For Bragg reflection we have $\lambda = 2d \sin \theta'$, and from simple geometrical considerations we can obtain

$$\lambda = \frac{2dD}{L} \cdot \frac{\sin^2 \alpha}{(\sin^2 \alpha + \sin 2\theta \sin 2\alpha + 4 \sin^2 \theta \cos^2 \alpha)^{1/2}}$$

Now the distance moved along the rack is directly proportional to wavelength, i.e. $\lambda = KD$

$$\text{Hence } K = \frac{\frac{2d}{L} \sin^2 \alpha}{(\sin^2 \alpha + \sin 2\theta \sin 2\alpha + 4 \sin^2 \theta \cos^2 \alpha)^{1/2}}$$

$$= \frac{\frac{2d}{L} \cos^2 \varepsilon}{(\cos^2 \varepsilon + \sin 2\theta \sin 2\varepsilon + 4 \sin^2 \theta \sin^2 \varepsilon)^{1/2}}$$

where $\alpha = \pi/2 - \varepsilon$

Now for small ε: $\cos^2 \varepsilon \longrightarrow 1$

$\sin^2 \theta \sin^2 \varepsilon \longrightarrow 0$ since θ is also small

and $\sin 2\theta \sin 2\varepsilon \longrightarrow 2\varepsilon \sin 2\theta$

Thus, $K \approx \frac{2d}{L}(1 - \varepsilon \sin 2\theta)$ expanding by the Binomial Theorem and ignoring higher order terms.

Consequently, K decreases as θ increases, which has been shown to be the case in the region above 200 kev. It is tentatively postulated, therefore, that the above misalignment takes effect as the source is moved out from the "zero" position until the strain experienced by the instrument is taken up by the bearing tolerences, after which K remains essentially constant.

The accuracy of certain other features of the alignment is also suspected. For example, the exact alignment of the centre spindle linking the source carriage to the

lower radial beam was extremely difficult to effect. The effect of a misalignment of this spindle on the performance of the machine is difficult to predict. It is possible, however, that a more accurate alignment of the spindle could decrease the peak width observed with the spectrometer.

A slight improvement could perhaps have been made in the alignment of the crystal clamping blocks. Although the curved crystal itself was accurately aligned, no means were provided whereby the alignment of the clamping blocks could be tested. After the blocks and crystal had been clamped to the mounting table, there was no longer any way to check the horizontal alignment of the table. For minimum peak width, the axis of the cylindrical profile of the blocks must be vertical. If the table supporting the clamping blocks was not horizontal, this would not be the case and consequently there should result a slight increase in peak width. The exact positioning of the centre of the crystal over the centre of the vertical shaft about which the radial beams pivot was also difficult to effect, and possibly added to the deterioration of the spectrometer performance.

The "humps" in the gamma-ray background curve observed with the spectrometer were originally thought to be largely due to some form of misalignment. A more satisfactory explanation, however, has been put forward. It is now firmly believed that these "humps" are simply a poorly resolved scintillation spectrum. When the source is close to the mechanical "zero" position of the spectrometer the majority of the radiation impinging upon the scintillating

crystal is due to the scattering of the direct beam down the collimator. As the source is moved out from the "zero" position the spectrum is simultaneously scanned by the scintillation spectrometer which would therefore detect two poorly resolved "humps" in the neighbourhood of the intense peaks in the spectrum. The almost constant background curve in the low energy region is due, of course, both to the lack of intense low energy gamma-rays, and to the fact that the collimator masks the direct beam much more efficiently in this region. This postulate could perhaps be verified by scanning the spectrum without the curved crystal. If it is correct, then an identical background curve should be produced with no lines imposed upon it, since the removal of the thin crystal lamina should have negligible effect upon the direct beam of radiation impinging upon the collimator. This experient cannot be performed at the present time, however, since it would entail a complete recalibration of the instrument.

The performance of the spectrometer driving assembly proved entirely satisfactory. Until tested, the linearity of the rack and pinion system was a major concern. The lack of scatter in the points on the wavelength calibration curve, however, reveals no periodicities or discontinuities in the rack performance. The machine will therefore prove very useful in the precise determination of gamma-ray energies. Indeed, the actual precision in the determination of gamma-ray wavelengths, which was discussed in the previous chapter, is much higher than was originally believed possible

due to the simplicity of the driving mechanism.

(II) GAMMA-RAY SPECTRUM OF Ir-192

The energies of the gamma-ray transitions following the decay of Ir-192 are very well known, and no new information has been established to-date using the calibrated curved crystal spectrometer. Some useful information however, has been gathered on the relative photon intensities of these transitions.

Since the effect of self-absorption in the source could not be taken into account, an empirical curve was drawn up in an attempt to resolve the radical disagreement between certain relative photon intensities determined by Baggerly and by Johns [see table (3)] . This curve takes into account the average of those relative photon intensities agreeing to within at least 20% which have been determined from two independent external conversion spectra and two independent curved crystal spectra. Thus, any errors inherent in either of the methods used to determine relative intensities should be considerably reduced. The majority of the points on this curve are correct to within 10% and further the points lie on a relatively smooth curve. It is conservatively estimated, therefore, that the intensities listed in column I of table (5) are correct to within 20%. Certainly this precision can be claimed for the relative photon intensities of transitions with energies greater than 200 kev. Below 200 kev. the curve has been extrapolated to include the 136 kev. transition. The relative photon intensity of this transition is therefore a little

more doubtful. The curve, however, appears to be flattening out which would seem to indicate that the effect of self-absorption is being compensated by the increased efficiency of the curved crystal. The value obtained for the relative photon intensity of the 136 kev. transition is identical with that of Dumond. If Johns' value were correct, a violent increase in the slope of the graph would have to occur between 200 kev. and 136 kev. This seems very improbable. The other relative photon intensities determined from the curve, all save the intensity of the 485 kev transition, agree to within 20% with the mean of the values quoted by Johns and by Dumond. For the 485 kev. transition the curve appears to indicate that the value quoted by Dumond is the more accurate.

BIBLIOGRAPHY

(1) Bragg, W.H. and Bragg, W.L. - Proc. Roy. Soc. A 88, 428 (1913)

(2) Frilley - C.R. Acad. Sci. Paris 186 137 (1928)

(3) Thibaud - C.R. Acad. Sci., Paris 180 138 (1925)

(4) Dumond and Kirkpatrick - Rev. Sci. Instrum. 1 88 (1930)

(5) Cauchois - C.R. Acad. Sci., Paris 194 362 (1932)

(6) Dumond - Rev. Sci. Instrum. 18,626 (1947)

(7) Dumond, Lind and Watson - Phys. Rev. 73 1392 (1948)

(8) Watson, West, Lind and Dumond - Phys. Rev. 75 505 (1949)

(9) Dumond, Lind and Watson - Phys. Rev. 75 1226 (1949)

(10) Lind, Brown, Klein, Muller and Dumond - Phys. Rev. 75 1544 (1949)

(11) Lind, Brown and Dumond - Phys. Rev. 76 1838 (1949)

(12) Baggerly, Marmier, Boehm and Dumond - Phys. Rev. 100 1364 (1955)

(13) Muller, Hoyte, Klein and Dumond - Phys. Rev. 88 775 (1952)

(14) Ewan - Ph.D. thesis, University of Edinburgh (1952)

(15) Ryde and Anderson - Proc. Phys. Soc. B, 68 1117 (1954)

(16) Simbaev - Soviet Physics J.E.T.P. vol. 5, no. 2, 170 (1957)

(17) Siegbahn (editor) - Beta and Gamma-Ray Spectroscopy, North-Holland Publishing Co., Amsterdam (1955) Chapter 4, page 102

(18) Kelman et al - Nuclear Physics 4 240 (1957)

(19) Huq - Il Nuovo Cimento 5 1456 (1957)

(20) Johns and Nablo - Phys. Rev. 96 1599 (1954)

(21) Bashilov, Antoneva, and Dzhelepov - Izv. Akad. Nauk SSSR Ser. Fiz. 16, 264 (1952)

(22) Mraz - Nuclear Physics 4 457 (1957)

(23) Kelly and Wiedenbeck - Phys. Rev. 102 1130 (1956)

(24) Mott and Sutton - Handbuch Der Physik XLV, 129 (1958)